

TI-860

9

ADA076046

WADC TECHNICAL REPORT 52-251, PART 1

DTIC

**INVESTIGATION OF COMPRESSIVE-CREEP PROPERTIES OF  
ALUMINUM COLUMNS AT ELEVATED TEMPERATURES**

R. L. CARLSON  
A. D. SCHWOPE

BATTELLE MEMORIAL INSTITUTE

Scanned by DTIC  
Date \_\_\_\_\_

SEPTEMBER 1952

Statement A  
Approved for Public Release

WRIGHT AIR DEVELOPMENT CENTER

## NOTICES

When Government drawings, specifications, or other data are used for any purpose other than in connection with a definitely related Government procurement operation, the United States Government thereby incurs no responsibility nor any obligation whatsoever; and the fact that the Government may have formulated, furnished, or in any way supplied the said drawings, specifications, or other data, is not to be regarded by implication or otherwise as in any manner licensing the holder or any other person or corporation, or conveying any rights or permission to manufacture, use, or sell any patented invention that may in any way be related thereto.

The information furnished herewith is made available for study upon the understanding that the Government's proprietary interests in and relating thereto shall not be impaired. It is desired that the Judge Advocate (WCJ), Wright Air Development Center, Wright-Patterson Air Force Base, Ohio, be promptly notified of any apparent conflict between the Government's proprietary interests and those of others.



**INVESTIGATION OF COMPRESSIVE-CREEP PROPERTIES OF  
ALUMINUM COLUMNS AT ELEVATED TEMPERATURES**

*R. L. Carlson  
A. D. Schwobe*

*Battelle Memorial Institute*

*September 1952*

*Materials Laboratory  
Contract No. AF 33(038)-9542  
RDO No. R614-13*

**Wright Air Development Center  
Air Research and Development Command  
United States Air Force  
Wright-Patterson Air Force Base, Ohio**

McGregor & Werner, Inc., Dayton, Ohio  
300 - February, 1953

## FOREWORD

This report was prepared by Battelle Memorial Institute, Columbus Ohio, under Contract No. AF 33(038)-9542. The contract was initiated under Research and Development Order No. 614-13, "Design and Evaluation Data for Structural Metals", and was initiated under the direction of the Materials Laboratory, Directorate of Research, Wright Air Development Center, with Mr. E. L. Horne acting as project engineer. This report covers work performed during the period 1 February 1950 to 30 September 1952.

The work accomplished in this study was performed by R. L. Carlson, Principal Mechanical Engineer, and A. D. Schwope, Supervisor.

ABSTRACT

An experimental investigation of the behavior of 24S-T4 (stabilized) aluminum columns at three elevated temperatures has been conducted. Tests were performed on long- and short-hinged-end columns of five slenderness ratios. By using an adjustable end eccentricity, it was possible to fix the eccentricity for a column of a given slenderness ratio and thereby obtain comparable results for different loads. Deflection measurements were taken at the mid-point throughout the duration of each test, and curves of deflection versus time with load as the parameter were obtained for each slenderness ratio. Test results indicate that, for a column of a given slenderness ratio and eccentricity, there is a limiting load below which collapse due to creep will not occur. It is concluded that this lower limit should be considered the limiting or allowable load. It is suggested that an approximate method of the type introduced in the report should be employed to determine this load.

PUBLICATION REVIEW

This report has been reviewed and is approved.

FOR THE COMMANDING GENERAL:

*M. E. Sorte*  
*for*  
M. E. SORTE  
Colonel, USAF  
Chief, Materials Laboratory  
Directorate of Research

TABLE OF CONTENTS

	<u>Page</u>
INTRODUCTION . . . . .	1
Material Selection . . . . .	1
Tests . . . . .	2
Test Specimens . . . . .	4
Tension Specimen . . . . .	4
Compression Specimen . . . . .	4
Column Specimens . . . . .	4
Equipment . . . . .	4
Tension-Static Tests . . . . .	4
Compression-Static Tests . . . . .	5
Tension and Compression Creep . . . . .	5
Column Tests . . . . .	7
Test Procedures . . . . .	13
Tension-Static Tests . . . . .	13
Compression-Static Tests . . . . .	13
Tension and Compression Creep . . . . .	14
Column Tests . . . . .	14
Test Results . . . . .	15
Tension-Static Tests . . . . .	15
Compression-Static Tests . . . . .	17
Tension and Compression Creep . . . . .	17
Column Tests . . . . .	26
Room Temperature . . . . .	26
300 F . . . . .	27
350 F . . . . .	27
450 F . . . . .	28
GENERAL DISCUSSION OF COLUMN CREEP . . . . .	34
The Creep Behavior of Perfect Columns . . . . .	34
The Creep Behavior of Imperfect Columns . . . . .	40
Use of Test Results . . . . .	41
Design Considerations . . . . .	49
REFERENCES . . . . .	52
APPENDIX I . . . . .	53
The Creep Behavior of Perfect Columns . . . . .	53
APPENDIX II . . . . .	58
Creep of an Imperfect Column . . . . .	58

LIST OF FIGURES

Figure 1. Tensile Stress-Strain Curves for 24S-T4 Aluminum Alloy . . . . .	3
Figure 2. Creep-Test Frame . . . . .	6
Figure 3. Compression-Creep Specimen . . . . .	9
Figure 4. Loading-Frame Unit . . . . .	10
Figure 5. Specimen and Furnace . . . . .	11
Figure 6. Transformer Assembly . . . . .	12
Figure 7. Tensile Stress-Strain Curves for Stabilized 24S-T4 Aluminum Alloy . . . . .	16

LIST OF FIGURES  
(Continued)

	<u>Page</u>
Figure 8. Variation of Yield Strength in Tension With Temperature . . . . .	18
Figure 9. Variation of Young's Modulus in Tension With Temperature . . . . .	18
Figure 10. Variation of Tangent Modulus With Stress in Tension . . . . .	19
Figure 11. Compressive Stress-Strain Curves for Stabilized 24S-T4 Aluminum Alloy . . . . .	20
Figure 12. Variation of Yield Strength in Compression With Temperature . . . . .	21
Figure 13. Variation of Young's Modulus in Compression With Temperature . . . . .	21
Figure 14. Variation of Tangent Modulus With Stress in Compression . . . . .	22
Figure 15. Tension- and Compression-Creep Curves for Stabilized 24S-T4 Aluminum Alloy Tested at 450 F . . . . .	24
Figure 16. Tension- and Compression-Creep Curves for Stabilized 24S-T4 Aluminum Alloy Tested at 350 F . . . . .	25
Figure 17. Total Deflection-Time Curves for Stabilized 24S-T4 Aluminum-Alloy Columns With L/r = 156, Tested at 350 F . . . . .	29
Figure 18. Total Deflection-Time Curves for Stabilized 24S-T4 Aluminum-Alloy Columns With L/r = 131, Tested at 350 F . . . . .	30
Figure 19. Total Deflection-Time Curves for Stabilized 24S-T4 Aluminum-Alloy Columns With L/r = 106, Tested at 350 F . . . . .	31
Figure 20. Total Deflection-Time Curves for Stabilized 24S-T4 Aluminum-Alloy Columns With L/r = 81.4, Tested at 350 F . . . . .	32
Figure 21. Total Deflection-Time Curves for Stabilized 24S-T4 Aluminum-Alloy Columns With L/r = 56.5, Tested at 350 F . . . . .	33
Figure 22. Total Deflection-Time Curves for Stabilized 24S-T4 Aluminum-Alloy Columns With L/r = 156, Tested at 450 F . . . . .	35
Figure 23. Total Deflection-Time Curves for Stabilized 24S-T4 Aluminum-Alloy Columns With L/r = 131, Tested at 450 F . . . . .	36
Figure 24. Total Deflection-Time Curves for Stabilized 24S-T4 Aluminum-Alloy Columns With L/r = 106, Tested at 450 F . . . . .	37
Figure 25. Total Deflection-Time Curves for Stabilized 24S-T4 Aluminum-Alloy Columns With L/r = 81.4, Tested at 450 F . . . . .	38
Figure 26. Total Deflection-Time Curves for Stabilized 24S-T4 Aluminum-Alloy Columns With L/r = 56.5, Tested at 450 F . . . . .	39
Figure 27. Column Load Versus Failure Time at Test Temperature of 350 F . . . . .	43
Figure 28. Column Load Versus Failure Time at Test Temperature of 450 F . . . . .	44
Figure 29. Critical Average Stress Versus Slenderness Ratio With Failure Time as a Parameter at Test Temperature of 350 F . . . . .	45
Figure 30. Critical Average Stress Versus Slenderness Ratio With Failure Time as a Parameter at Test Temperature of 450 F . . . . .	46
Figure 31. Critical Average Stress Versus Slenderness Ratio for Three Testing Temperatures . . . . .	48
Figure 32. Comparison of Limiting Average Stress Curves and Experimental Results . . . . .	51

LIST OF FIGURES  
(Concluded)

	<u>Page</u>
Figure 33. Loading Procedure on a Critical Average Stress Versus Slenderness Ratio Diagram . . . . .	54
Figure 34. Loading Procedure on a Stress Versus Strain Diagram . . . . .	54
Figure 35. The Column Configuration . . . . .	59
Figure 36. A Column Section . . . . .	59
Figure 37. Initial Stress Distribution . . . . .	61
Figure 38. Change in Strain Due to Creep . . . . .	61
Figure 39. Elastic Adjustment to Obtain Plane Sections . . . . .	63
Figure 40. Elastic-Strain Change to Obtain Plane Sections . . . . .	63
Figure 41. Elastic-Axial-Stress Adjustment . . . . .	64
Figure 42. Elastic-Axial-Strain Adjustment . . . . .	64
Figure 43. Elastic-Bending-Stress Adjustment . . . . .	67
Figure 44. Elastic-Bending-Strain Adjustment . . . . .	67
Figure 45. Initial and Final Stress Distributions . . . . .	69
Figure 46. Initial and Final Strain Distributions . . . . .	69

# INVESTIGATION OF COMPRESSIVE-CREEP PROPERTIES OF ALUMINUM COLUMNS AT ELEVATED TEMPERATURES

## PART I

### INTRODUCTION

The use of materials in aircraft applications in which temperature effects must be considered is becoming increasingly more common. In many instances, the temperatures have become sufficiently high to enable time-dependent deformation or creep to take place. As a consequence, the usual stress and deformation solutions based on the theories of elasticity and plasticity no longer adequately describe the structural behavior to be expected.

In some of the applications in which creep occurs, it has been common practice to ignore the effect of the transient component of creep and to consider only the steady-state component. Often such a treatment is satisfactory. For example, it has been observed experimentally that, in the bending of beams by creep, a steady-state condition (the rate of deflection becomes constant) often is reached after a short period of time. In such instances, a steady-state type of solution is permissible if the amount of deflection resulting from the transient component is small compared with the amount of steady-state deflection occurring over a long period of time.

In the above example, two conditions made the steady-state type of solution permissible. One was that it was necessary that a steady-state condition be reached, and the other was that relatively long periods of time be involved. Needless to say, there are many situations in which these requirements are not satisfied. One such situation which is of immediate practical importance is in the study of columns which are subject to creep.

Although a few theories<sup>(1, 2, 3)</sup> have been proposed in recent years to describe the column action during creep, little experimental data have been obtained which provide a means of verifying the proposed theories. One of the purposes of the investigation covered by this report was to provide a complete set of data from columns with several slenderness ratios for a given material (24S-T4 (stabilized) aluminum). A further purpose was to determine from an analysis of the experimental results what methods might be best suited for predicting column-creep behavior by the consideration of easily obtained material properties.

### Material Selection

The test material selected for this investigation was 24S-T4 (stabilized) aluminum alloy. Originally, it was intended to use an extruded form

of rectangular 1/4- by 1/2-inch cross section of this alloy, but it was discovered that dimensional nonuniformity made this choice unsuitable, and a new selection was necessary. The form finally selected was cold-rolled stock of circular cross section. It was found that stock of this form could be machined to 1/4- by 1/2-inch cross-section column specimens with a dimensional variation of less than 0.001 inch.

Early in the investigation, it was decided that the results of the investigation could be more easily interpreted if no appreciable metallurgical transformations were taking place during the tests. With this in mind, it was decided that test specimens should be stabilized, and, from previous experience, a stabilization temperature of 600 F and a stabilization time of 100 hours were adopted.

To determine the effect of the stabilization on the material properties, room-temperature tensile tests were performed on two stabilized specimens and compared with tests performed on two "as-received" specimens. The results of these tests are given in Figure 1. From these curves, it can be seen that although the change in Young's modulus due to stabilization is not great, the stress necessary to initiate plastic flow is markedly reduced.

Since the tests conducted in the investigation required that specimens be exposed to temperatures of 350 F and 450 F for periods of time to 200 hours, a test was conducted to determine the effect of prior stabilization on specimens exposed to such conditions. In Figure 1, it can be seen that the tensile properties of a stabilized specimen that was heated at 450 F for 200 hours prior to testing were not significantly changed. As a consequence, it was concluded that this stabilization treatment essentially eliminated any metallurgical changes. All subsequent data presented in this report has been obtained on 600 F stabilized material.

### Tests

The tests conducted as a part of this investigation were as follows:

1. Tension and compression static tests at 450 F, 350 F, and room temperature. The purpose of these tests was to determine the variation of the material properties with temperature. A further purpose was to obtain at each test temperature the variation of the tangent modulus with stress.
2. Tension and compression-creep tests. These tests were conducted to determine creep characteristics at 450 F, 350 F, and room temperature in the stress range encountered in the column testing.

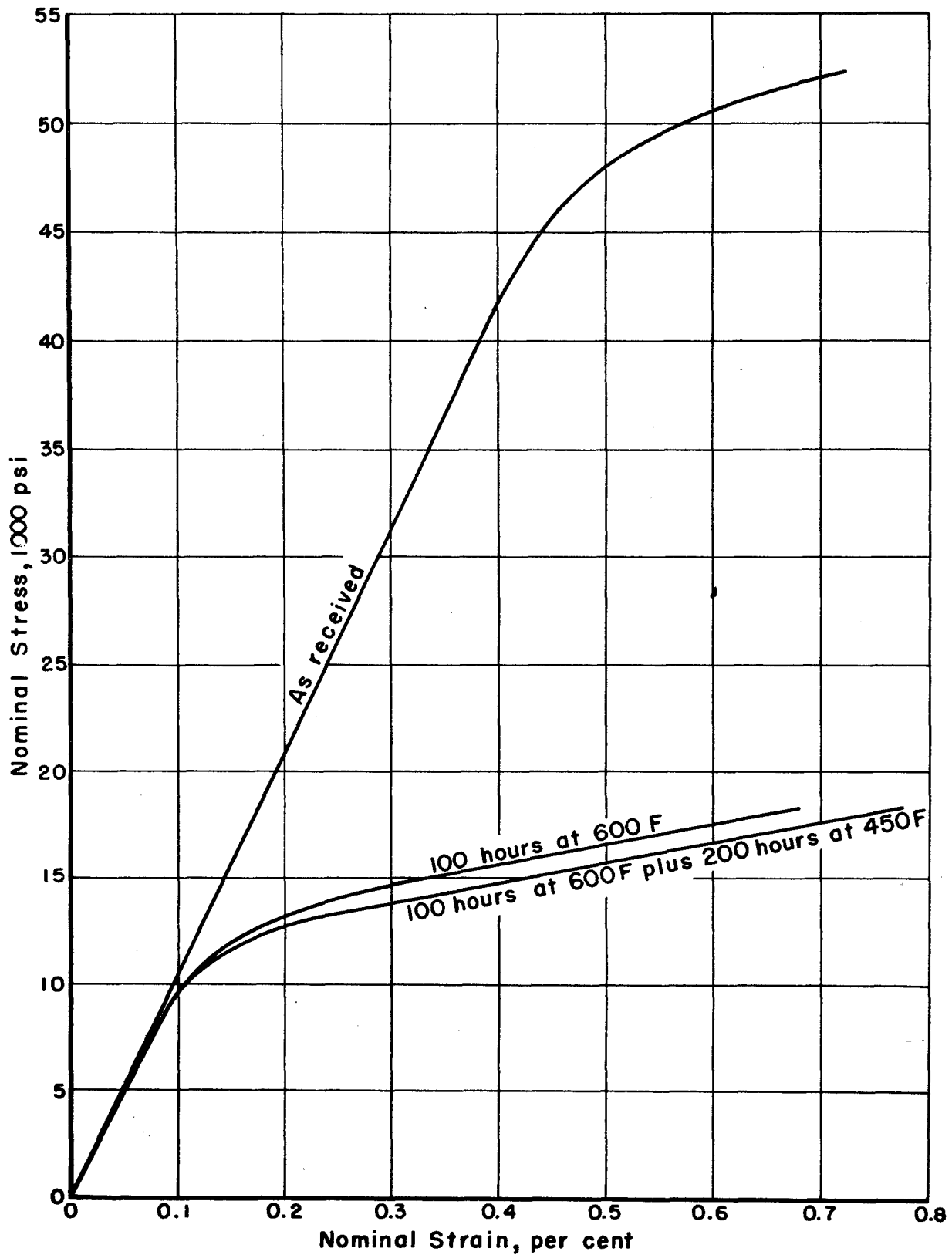


FIGURE I. TENSILE STRESS-STRAIN CURVES FOR 24S-T4 ALUMINUM ALLOY

3. Column tests at 350 F, 450 F, and room temperature. These tests were performed to investigate the variation of critical average stress with slenderness ratio for different failure times at each test temperature.

A more detailed description of each of these tests is given in the section of this report on testing procedures.

## Test Specimens

### Tension Specimen

Specimens of the same design were used for both the tension-static tests and the tension-creep tests. The design of these specimens was essentially that recommended by the ASTM for round tension specimens. The gage length was 2 inches and the cross-sectional area was 0.125 square inch.

### Compression Specimen

The first compression tests, both static and creep, were conducted on specimens which were 1.1 inches long, 0.5 inch wide, and 0.25 inch thick. As will be discussed later, however, the results obtained with this specimen for creep testing indicated that the design was unsatisfactory, and a specimen of different design was tried. This specimen, which had a circular cross section of 0.500-inch diameter, and a length of 1.75 inches, was then used to perform both the static- and creep-compression tests.

### Column Specimens

The column specimens were designed to give five slenderness ratios ranging from 56.5 to 156. This was achieved by holding the cross-sectional area constant and varying the length. For simplicity sake, a rectangular section of 1/4 inch by 1/2 inch was chosen. The column lengths including the end caps were then selected as 4.1, 5.9, 7.70, 9.15, and 11.3 inches.

## Equipment

### Tension-Static Tests

A universal hydraulic testing machine equipped with grips to accommodate the threaded ends of the specimen was used to perform the tensile

tests. A split furnace was used to obtain the elevated test temperatures and a control of temperature was accomplished by the use of a Foxboro temperature controller. A control iron-constantan thermocouple was attached to the center of the gage section of the test specimen.

Strain measurements during each test were obtained by the use of two Baldwin AB-3 high-temperature strain gages which were fixed to opposite sides of the specimen in the gage section. In order to compensate for temperature, dummy gages were fixed to bars of 24S-T4 (stabilized) aluminum which in turn were attached to the specimen grips. Each dummy gage was within 1/4 inch of its corresponding active gage.

### Compression-Static Tests

Compression tests were performed by the use of a subpress which was placed on the bed of a universal hydraulic testing machine. The design of the subpress was essentially of the type recommended by the ASTM Method B 9-46 T.

A split furnace was used to obtain the elevated test temperatures and a control of temperature was accomplished by the use of a Foxboro temperature controller. A control iron-constantan thermocouple was attached to the center of the gage section.

Strain measurements during each test were obtained by the use of three Baldwin AB-3 high-temperature strain gages which were fixed to the specimen at intervals of 120 degrees. Space limitations made the use of more than two dummy gages impossible, hence, a switching arrangement was utilized to make use of the three active gages. A detailed explanation of how this arrangement was used is given in this report in the section on testing procedure.

### Tension and Compression Creep

Both the tension-creep and compression-creep specimens were loaded by a dead-weight, lever-arm type of test frame as shown in Figure 2. In the case of the tension specimen, the load was transmitted as a tension, whereas in the case of the compression specimen a tensile load was converted to a compressive force by means of cage-type jig. With this one exception, the equipment for these two tests was essentially the same.

To obtain the test temperature, a sleeve-type furnace was used, and temperature control was accomplished by means of a thermocouple and Foxboro arrangement.

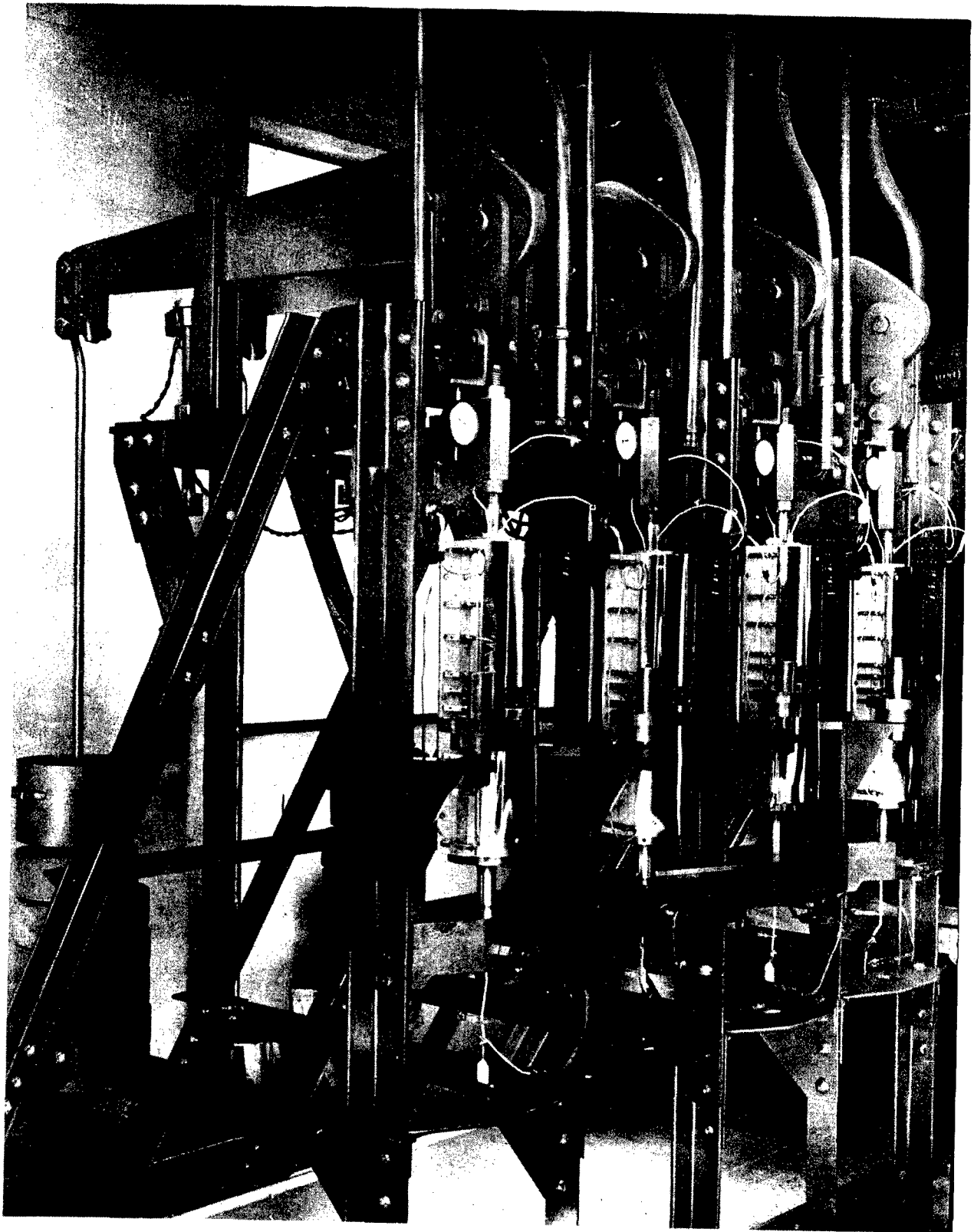


FIGURE 2. CREEP-TEST FRAME

The strain readings for both tension- and compression-creep tests were obtained by noting the relative movement of intersliding platinum strips through a microscope. Two strip units were used on each specimen, and they were mounted opposite one another. Figure 3 shows the cylindrical compression specimen with the platinum strips as it was mounted in the compression jig.

For the 1.1-inch-long rectangular specimen, the strips were attached near the specimen ends and gave a gage length of approximately 0.75 inch. The 1.75-inch-long cylindrical specimen also had the strips attached near the specimen ends, and the gage length was approximately 1.4 inches. For the tension specimens, the strip ends were attached to the edges of the specimen shoulders next to the fillets. The effective gage length was then taken to be the distance between the bottoms of the fillets. This distance was 2.25 inches. Although it might appear that this procedure would give values of unit strain that would be high, it has been found from experience that the error introduced is slight, since the amount of deformation that takes place between the fillet bottom and the shoulder edge is relatively small.

### Column Tests

The principle parts of the test equipment used for this section of the testing program consisted of the loading frame, the furnace, and the deflection recorder. Figure 4 shows a loading-frame unit with a test column in the testing position. The more important parts of the unit are as follows:

1. The overhead lever arm at the top of the picture transmits the load from a loading pan attached to the left end of the arm through two hardened-steel knife edges. For the arrangement as shown, the ratio of the specimen load to the pan load is 21 to 1.
2. The split furnace. It is shown in an open position. A 0-130 volt Variac was used to adjust the voltage input to the furnace.
3. The hinged-end column specimen. The column shown is a tested column. The amount of permanent bow in tested columns is, of course, determined by the amount that the lever arm is allowed to drop after collapse. The screw in the upper left corner is used to support the lever arm after the collapse of the column.
4. The control-thermocouple clamp is attached slightly above the center of the column. The thermocouple used was of the iron-constantan type, and control was accomplished by the use of a Foxboro temperature controller.

5. The yoke attached to the center of the column is connected to a quartz rod which in turn is fixed to a core passing through a transformer coil. The details of the transformer assembly are more clearly illustrated in the drawing of Figure 6.

Figure 5 is a close-up of the test specimen and the furnace. In this picture, the discs at the top and bottom are Transite end heaters designed to reduce the heat loss due to conduction through the plungers. Also to be noted in this figure are the knife-edge end caps and the steel shims used to adjust end eccentricity.

The utilization of an Atcotran linear differential transformer (Figure 6) to measure deflections was accomplished by transmitting the column movement to the transformer core by means of the quartz tube. The core in turn passes through coils consisting of a primary into which a 6-volt 60-cycle signal is fed, and two equal secondary windings placed so that the one is 180 degrees out of phase with the induced voltage of the other. If the core is so positioned that the induced voltage of both coils is equal, the net voltage output is zero. If, however, the core moves from this position, the induced voltages of the two coils will not be equal and the voltage output will be the difference between them. For the tests conducted, the voltage output is fed into a Brown-Honeywell three-channel recorder whose scale is calibrated in terms of core movement, which is a measure of the deflection of the column.

A calibration of the recorded movement against the core movement of 0.1 inch as measured by a depth micrometer was made, and the error was found to be less than 1.3%. This calculation was based on the assumption that the micrometer had an accuracy of 0.0001 inch in 0.1 inch movement. Since a plot of the calibration points measured at 0.002-inch intervals was linear, it can be assumed that the error within the 0.1-inch range was also less than 1.3%.

For the testing program conducted, there were three loading-frame units of the type in Figure 4. The only difference in these units was in the length dimension of the rods which support the top plate of the frame. Three different lengths were made to accommodate the various specimen lengths tested.

In a temperature calibration in which thermocouples were embedded in dummy specimens, it was found that the temperature variation along the lengths was plus or minus 3 F at a temperature of 450 F. During the tests, the Foxboro temperature controller enabled the temperature to be held within plus or minus 5 F.



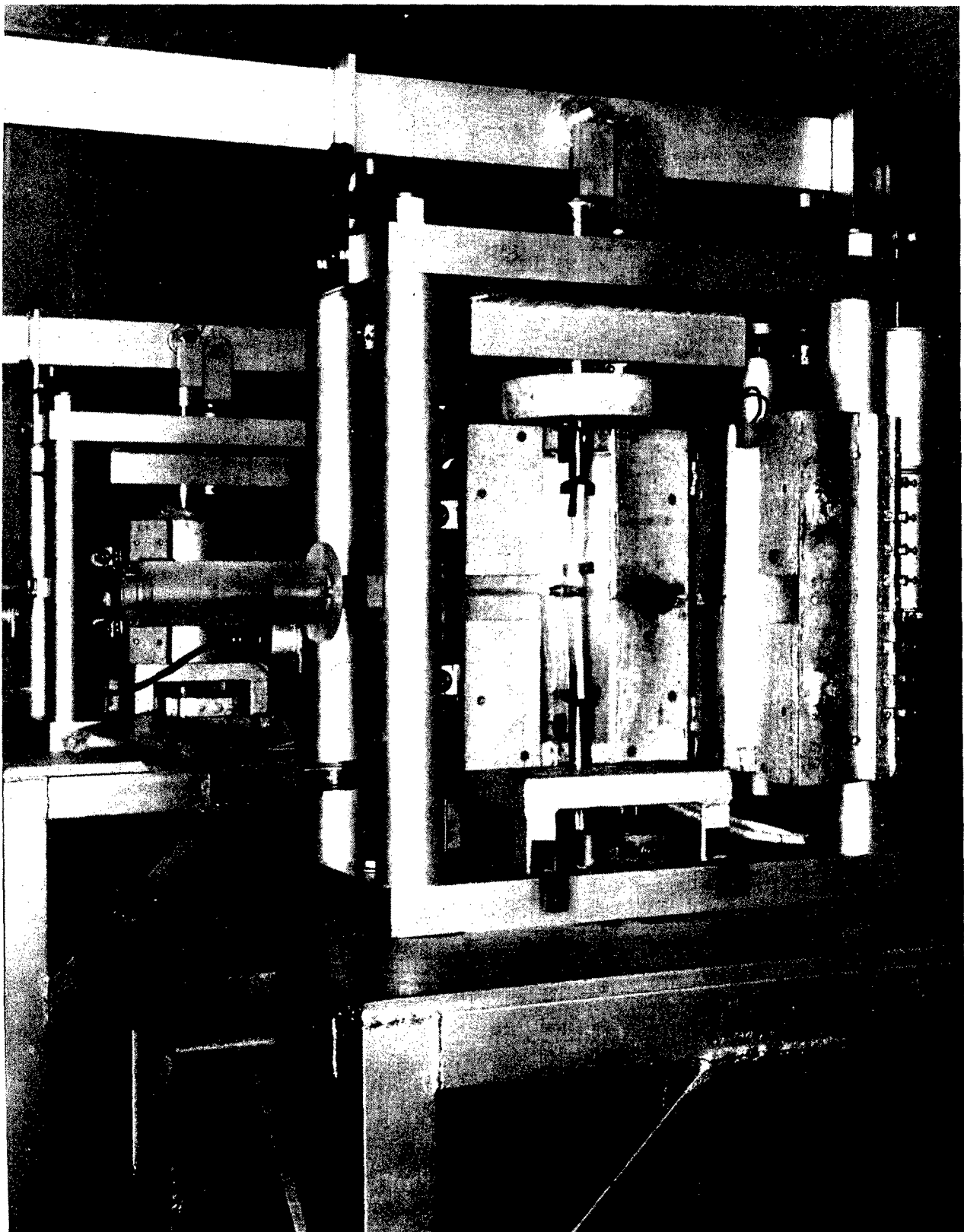


FIGURE 4. LOADING-FRAME UNIT

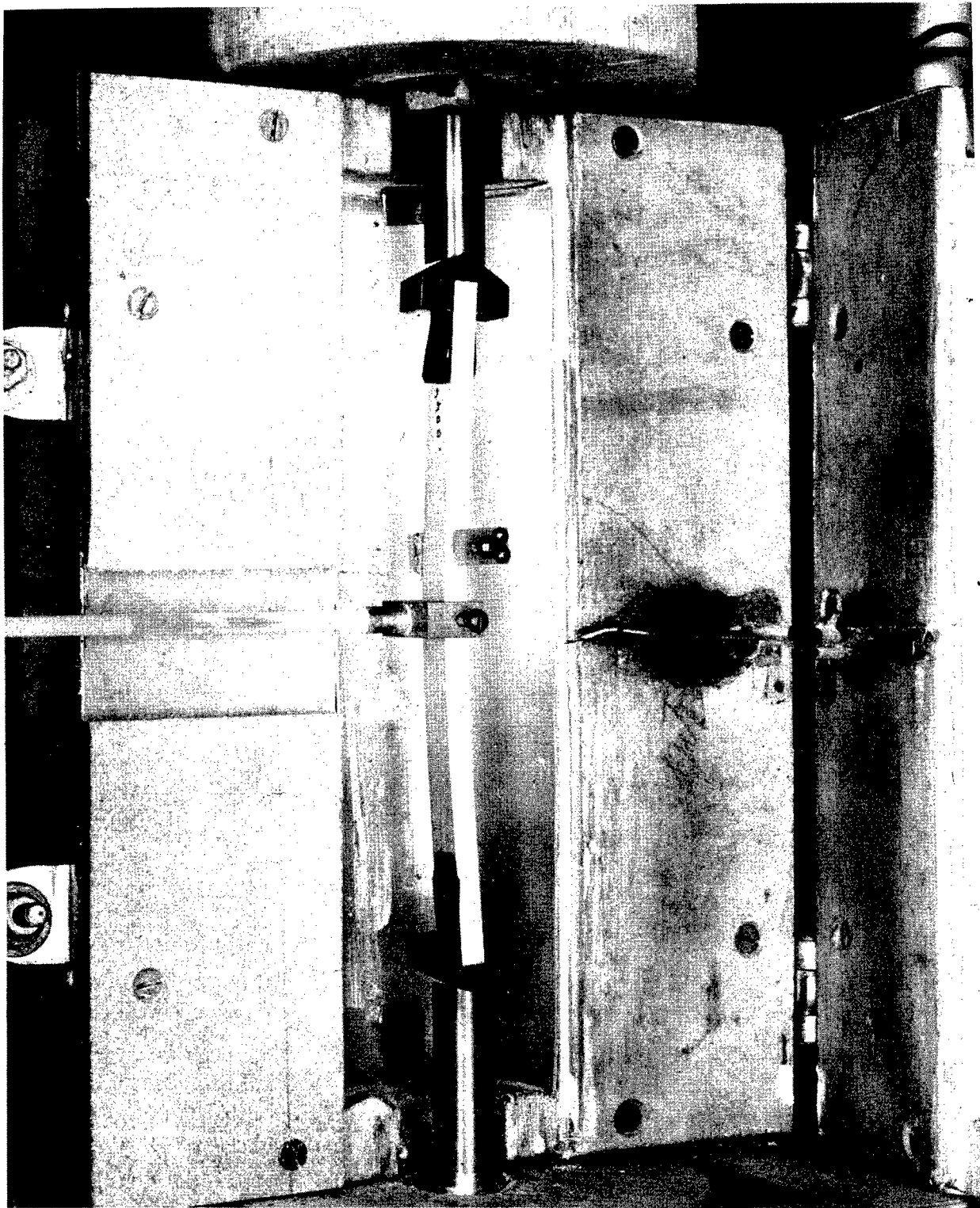


FIGURE 5. SPECIMEN AND FURNACE

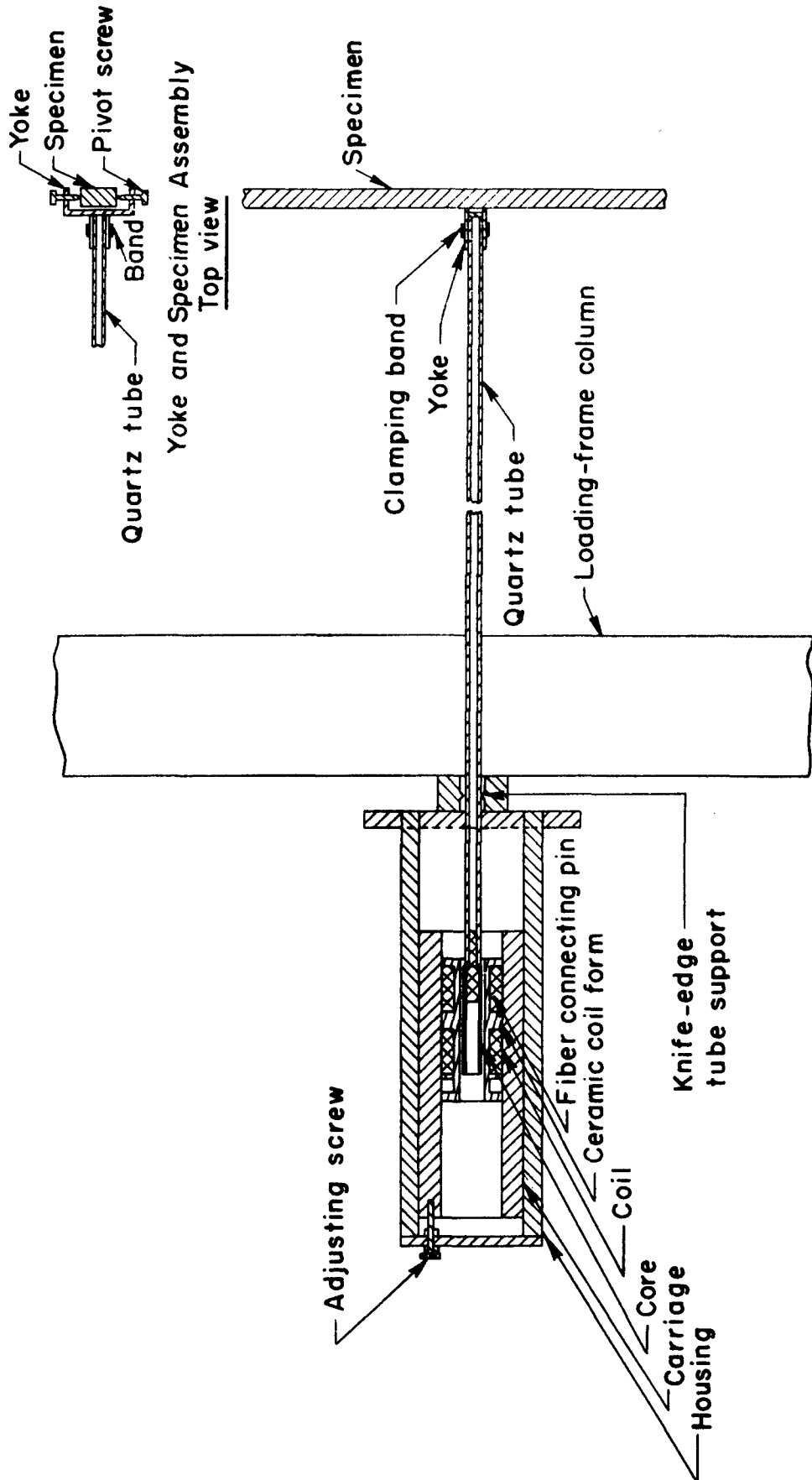


FIGURE 6. TRANSFORMER ASSEMBLY

## Test Procedures

### Tension-Static Tests

The test procedure for room-temperature tests and elevated-temperature tests was the same except for the use of a furnace in the case of the latter. As a consequence, only the elevated-temperature-test procedure will be described.

The procedure used consisted of first loading the specimen elastically at room temperature to make certain that alignment was satisfactory. The furnace was then slipped on and the specimen was heated to the test temperature. After reaching the test temperature, approximately one hour was allowed to pass before testing to assure stable conditions. The test was then conducted at a head speed of 0.005 inch per minute and readings were taken from both strain gages at 50-pound intervals.

Since the gage factor of the AB-3 decreases slightly with increasing temperatures, the manufacturers' stated value was not used. Instead, the values reported by Day<sup>(4)</sup>, given below, were used:

<u>Test Temperature,</u> <u>F</u>	<u>Gage</u> <u>Factor</u>
75	2.08 (Manufacturers' value)
350	2.07
450	1.94

### Compression-Static Tests

The procedure used for compression testing consisted of first loading the specimen elastically at room temperature to assure satisfactory alignment. Since the specimen had a circular cross section, it was necessary to use three strain gages at intervals of 120 degrees.

After reaching the test temperature, approximately one hour was allowed to pass before testing to assure stable conditions.

As was noted previously in the section on equipment, space limitations made the use of more than two dummy gages impossible. Since the use of the three actives was felt desirable for an elastic modulus determination, a switching arrangement was used to make this possible. After determining the modulus, the specimen was unloaded, and then, using only two gages, the test was conducted to completion at a head speed of 0.005 inch per minute.

## Tension and Compression Creep

The procedure used for tension- and compression-creep testing was to check the alignment at room temperature before heating the specimen to temperature.

When the specimen had become stable at the test temperature, the unloaded readings were taken. The specified load was then gradually applied to the lever arm, and the zero time readings were taken. Enough subsequent readings were taken during the test period to establish the creep versus time behavior.

## Column Tests

Two of the most common imperfections which make actual columns differ from ideal columns are an eccentricity of load application and the presence of an initial curvature. In the column-testing program conducted, it was desirable that these imperfections be as nearly the same as possible for a given column length. If this could not be achieved, a comparison of the results of tests for the given length would be extremely difficult. Since it is not likely that columns chosen at random will have these imperfections to the same degree, it was decided to arbitrarily select in advance the degree of imperfection, and to adjust each column to fit the choice.

Fortunately, the maximum deflection,  $\delta$ , caused by the load,  $P$ , can be represented<sup>(7)</sup> by

$$\delta = \left( \alpha + \frac{4e}{\pi} \right) \frac{1}{\frac{P_c}{P} - 1} ,$$

where

$\alpha$  is maximum unloaded deflection due to curvature,

$e$  is the amount of eccentricity of loading at both ends, and

$P_c$  is the critical load for a perfect column of the given length.

With this formula in mind, the end caps for the columns were made to allow for end-eccentricity adjustments by the use of shims (see Figure 5). According to this procedure, an effective eccentricity,  $C$ , is defined as

$$C = \alpha + \frac{4e}{\pi} .$$

Since it is logical to assume that this imperfection should be a function of the column length, a value of

$$C = \frac{L}{1200}$$

was selected.

Making use of the above ideas, the following testing procedure was developed for column tests:

1. Shim adjustments were made at the column ends until the column deflected according to the formula

$$\delta = \frac{C}{P_c/P - 1}$$

where

$$C = \frac{L}{1200}$$

The deflections corresponding to several loads were checked, and care was observed to make certain the column did not deform permanently.

2. The column was enclosed by the loading-frame furnace, and heated to the test temperature.
3. After allowing the column to become stabilized at the test temperature, the load to be used was applied as smoothly and rapidly as possible. The time,  $t = 0$ , for the creep test was that time at which the specified load was completely applied.
4. Deflection readings were printed by the recorder every 45 seconds for the duration of the test.

### Test Results

#### Tension-Static Tests

Tension-static tests were conducted according to the procedure given in the previous section for test temperatures of 450 F, 350 F, and room temperature. The results of these tests are given in the form of stress-strain curves in Figure 7. Each curve shown is the plotted average of two tests. In all cases, if the agreement between the first two tests conducted was not good, a third test was conducted, and the two tests giving the best agreement were used. In most instances, however, two tests were sufficient.

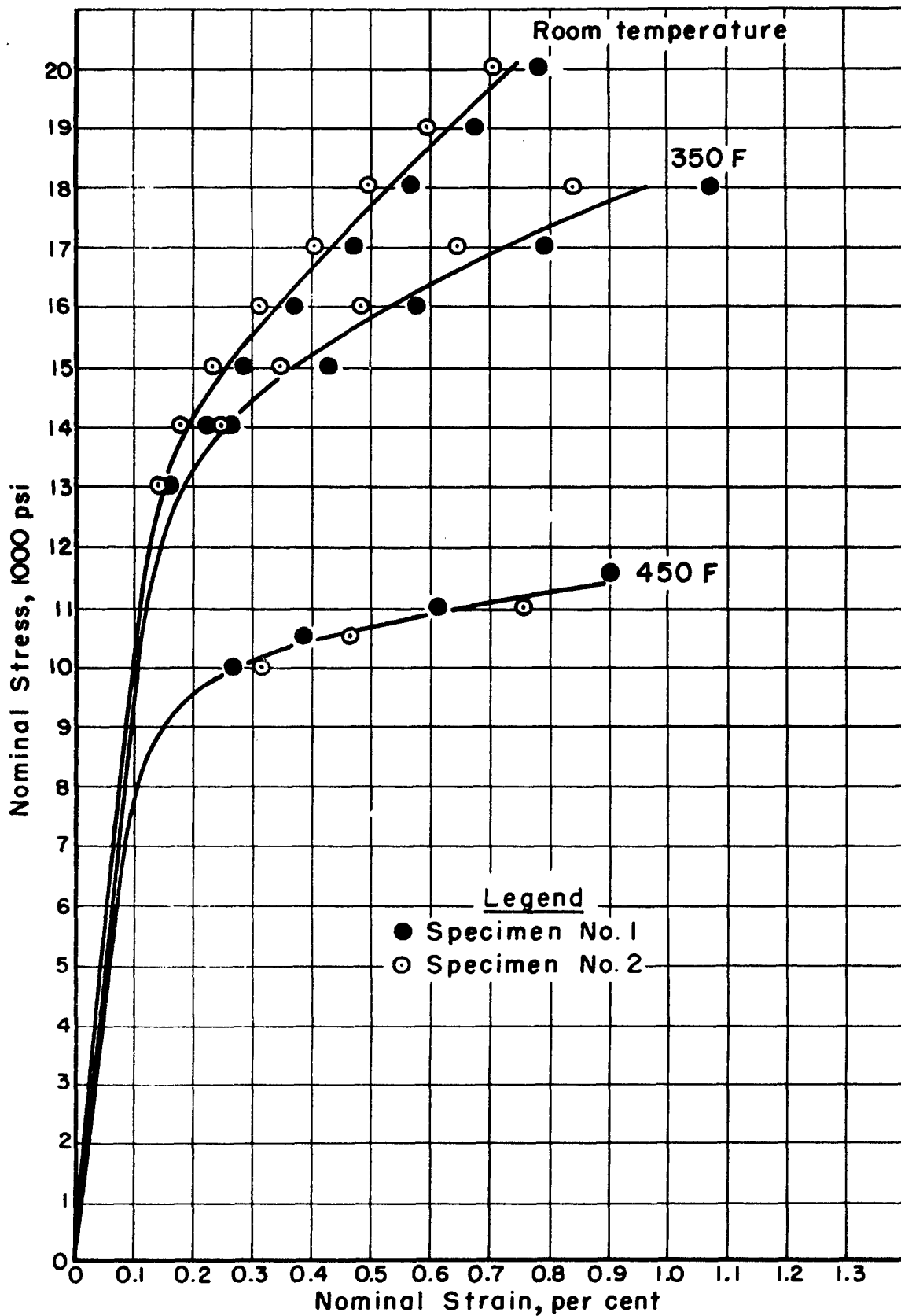


FIGURE 7. TENSILE STRESS - STRAIN CURVES FOR STABILIZED 24S-T4 ALUMINUM ALLOY

To illustrate the variation of yield strength and Young's modulus with test temperature, the curves of Figures 8 and 9 were constructed. It will be noted that, though the decrease in Young's modulus is not too marked in the test temperature range, the decrease in the yield strength is quite marked beyond approximately 300 F. This merely indicates that the principle effect of the temperature increase is to lower the stress necessary to produce plastic flow.

As another indication of the effect of test temperature, the tangent modulus versus stress curves for the test temperatures are given in Figure 10. For these curves, the plotted points give the values of stress for which tangents were determined from the respective stress-strain curves.

### Compression-Static Tests

Compression-static tests were conducted according to the procedure given in the previous section for test temperatures of 450 F, 350 F, and room temperature. The results of these tests are given in the form of stress-strain curves in Figure 11. Each curve shown is the plotted average of two tests.

To illustrate the variation of yield strength and Young's modulus with test temperature, the curves of Figures 12 and 13 were constructed. As was the case in tension, it will be noted that, although the decrease in Young's modulus is not too marked in the test-temperature range, the decrease in yield strength is rapid beyond approximately 300 F.

In Figure 14, the variation of tangent modulus with stress is given. The plotted points represent values calculated from the respective stress-strain curves. A comparison of these curves with those obtained for tension reveals that, in general, as would be expected, the value of the tangent modulus corresponding to a given value of stress is higher for compression than for tension. The one exception to this tendency is for an upper portion of the curves for 450 F. The reversal in this instance is within the probable experimental error, however, and it is felt that it does not represent the true trend.

For this investigation, the principle use of the compression tangent modulus versus stress curves was for the calculation of column tangent modulus and reduced modulus curves for each test temperature.

### Tension and Compression Creep

One of the primary concerns of this portion of the investigation was to determine whether or not tension- and compression-creep properties were sufficiently alike in the stress range of interest to permit the use of tensile-creep data in the analysis of column-creep considerations.

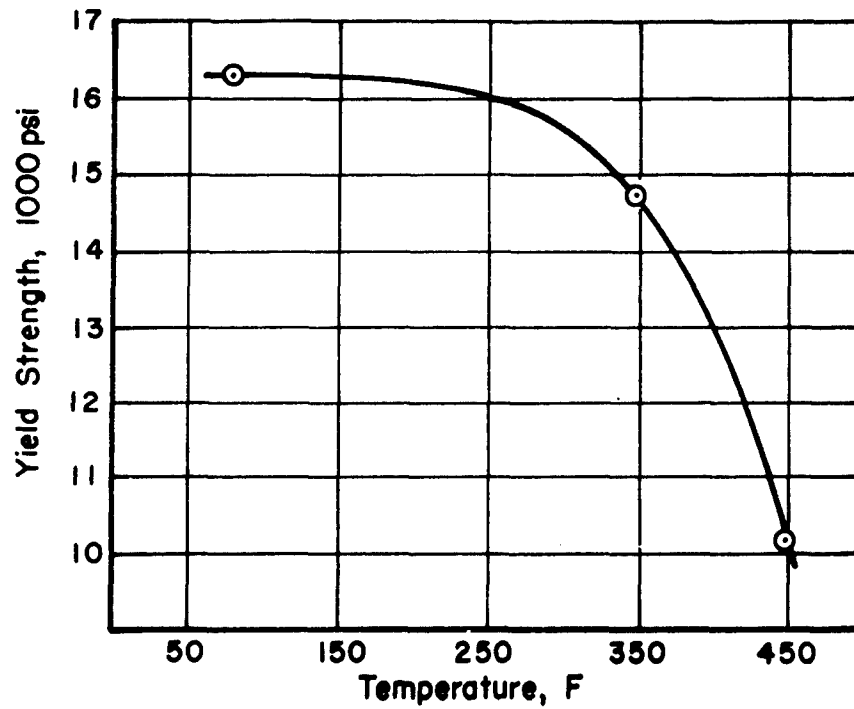


FIGURE 8. VARIATION OF YIELD STRENGTH IN TENSION WITH TEMPERATURE

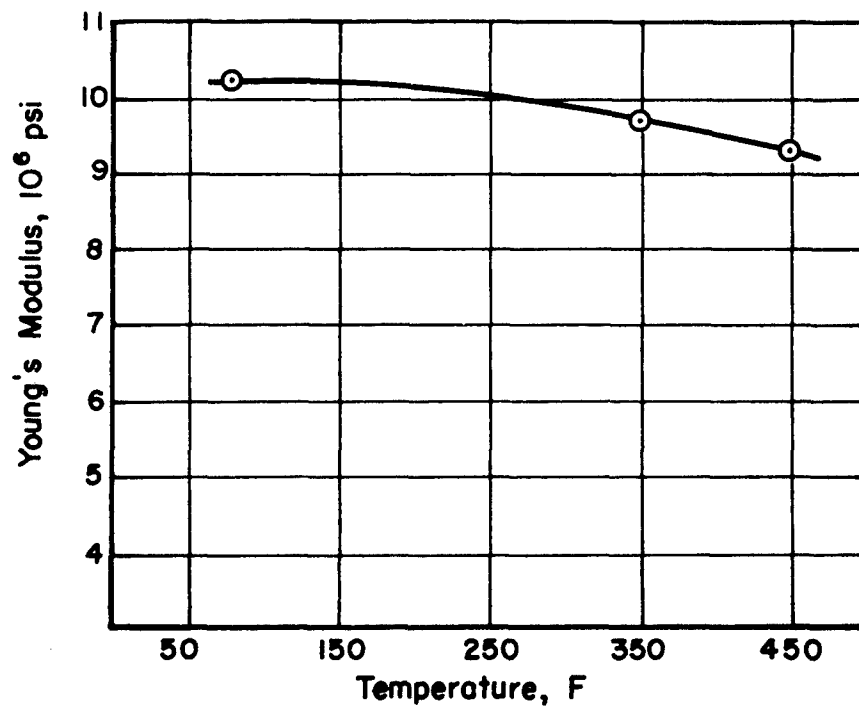


FIGURE 9. VARIATION OF YOUNG'S MODULUS IN TENSION WITH TEMPERATURE

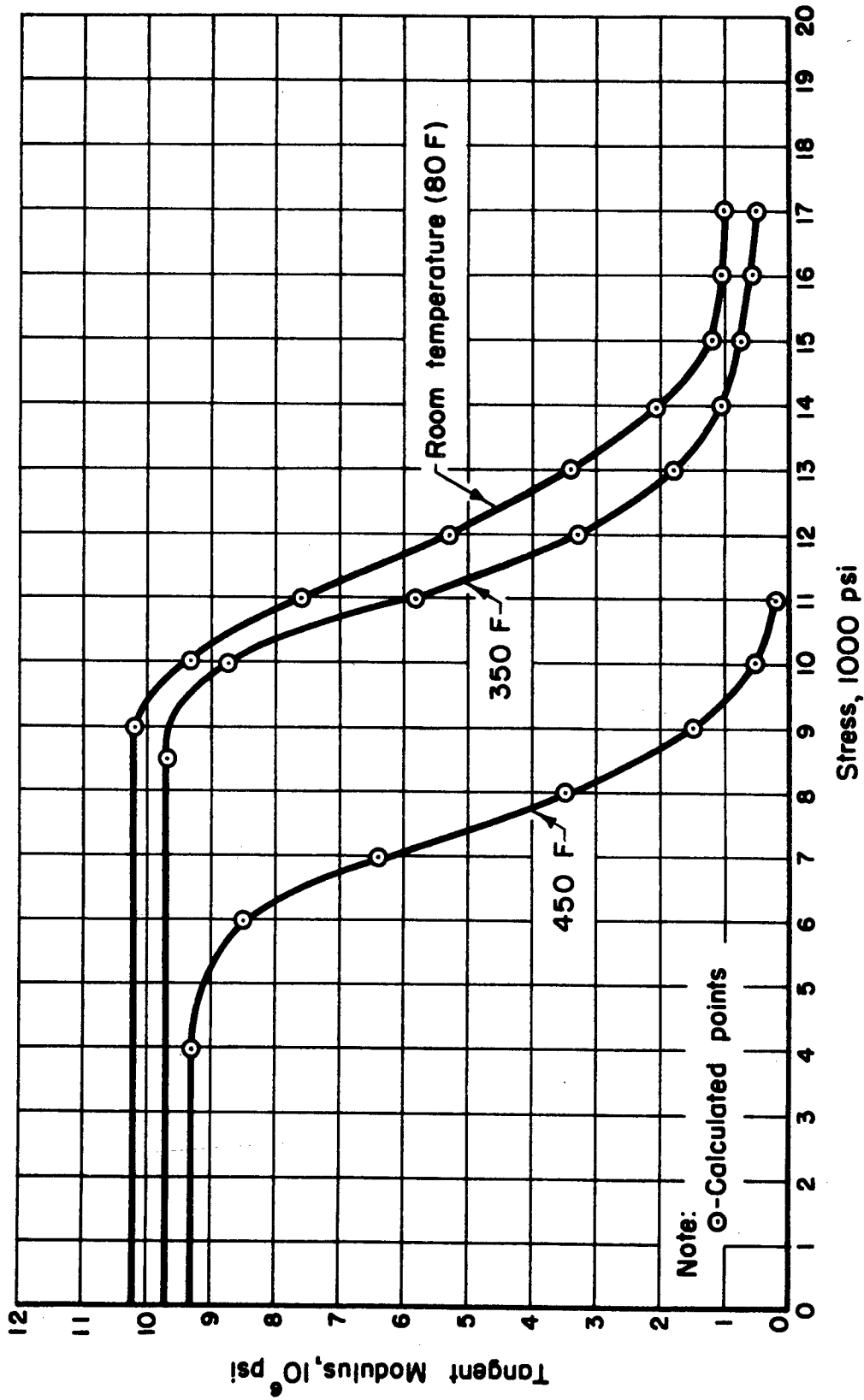


FIGURE 10. VARIATION OF TANGENT MODULUS WITH STRESS IN TENSION

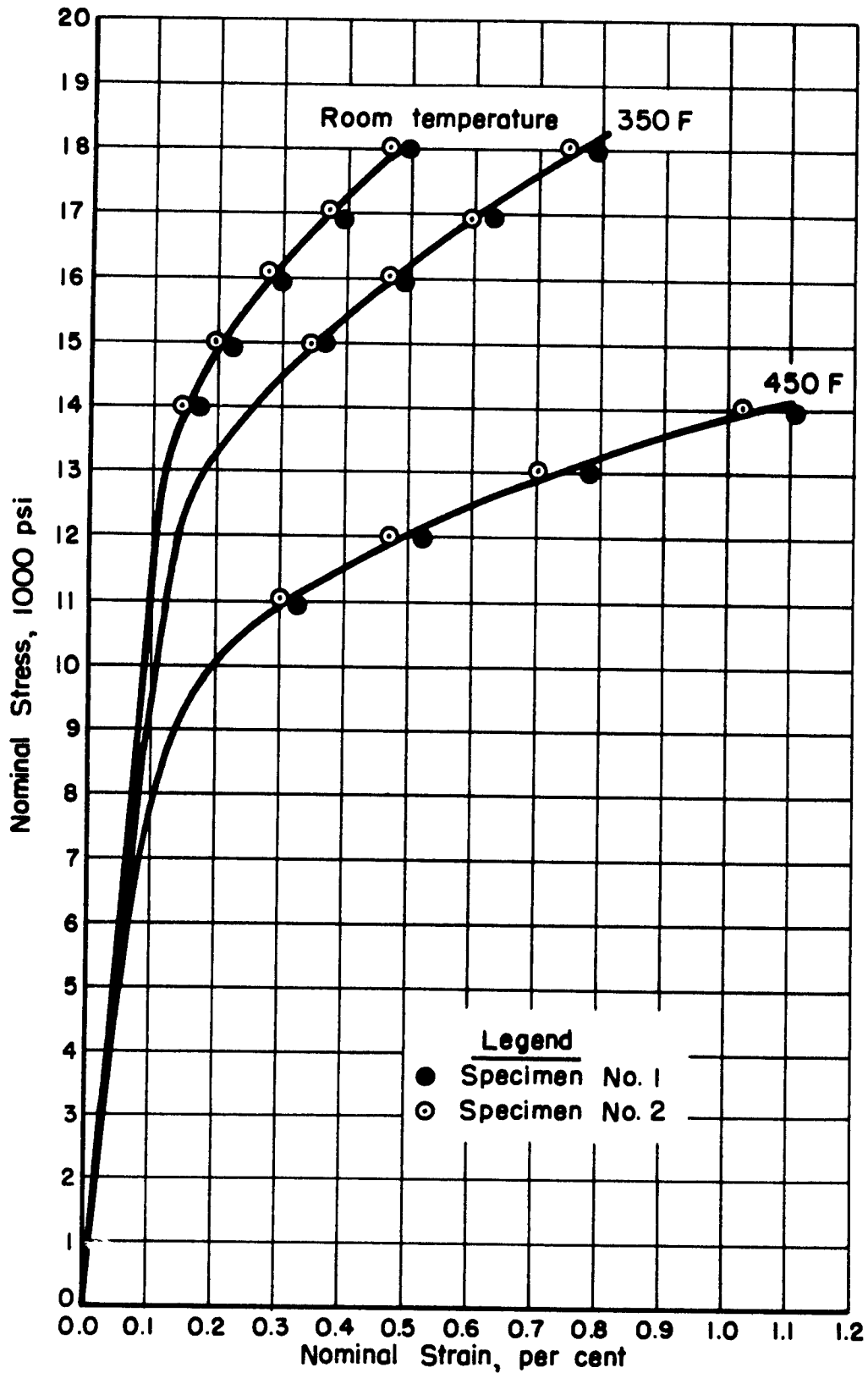


FIGURE II. COMPRESSIVE STRESS-STRAIN CURVES FOR STABILIZED 24S-T4 ALUMINUM ALLOY

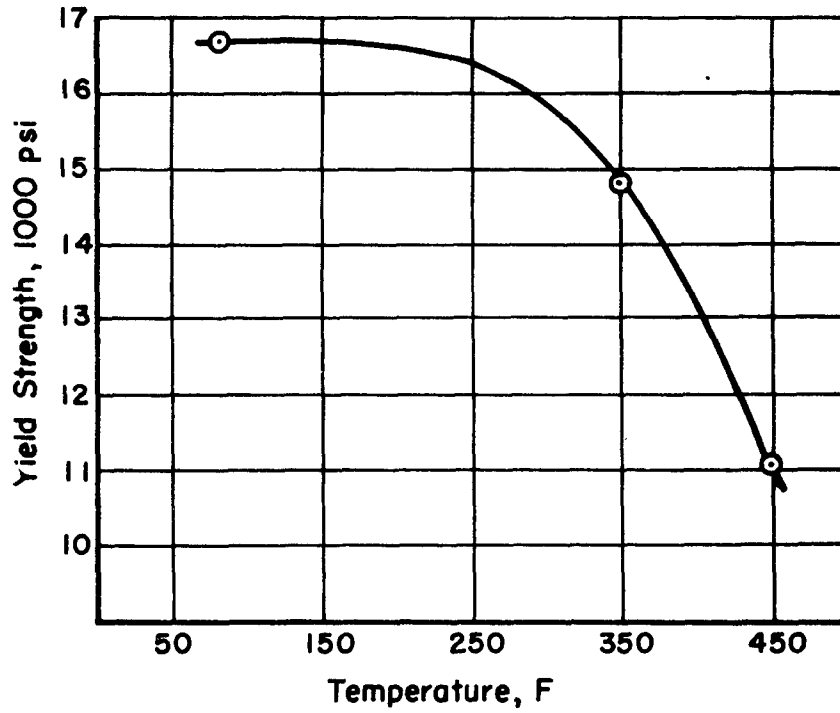


FIGURE 12. VARIATION OF YIELD STRENGTH IN COMPRESSION WITH TEMPERATURE

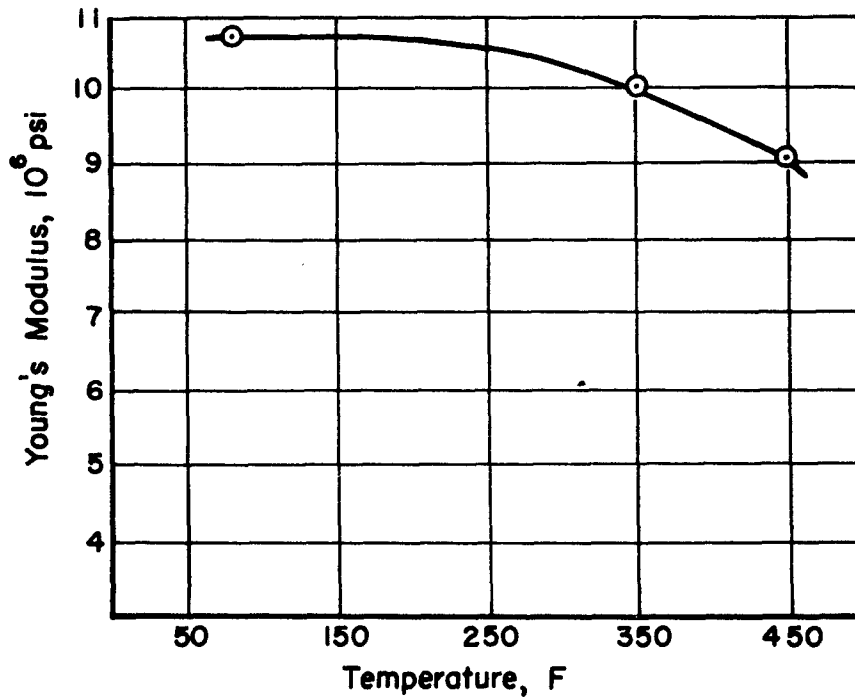


FIGURE 13. VARIATION OF YOUNG'S MODULUS IN COMPRESSION WITH TEMPERATURE

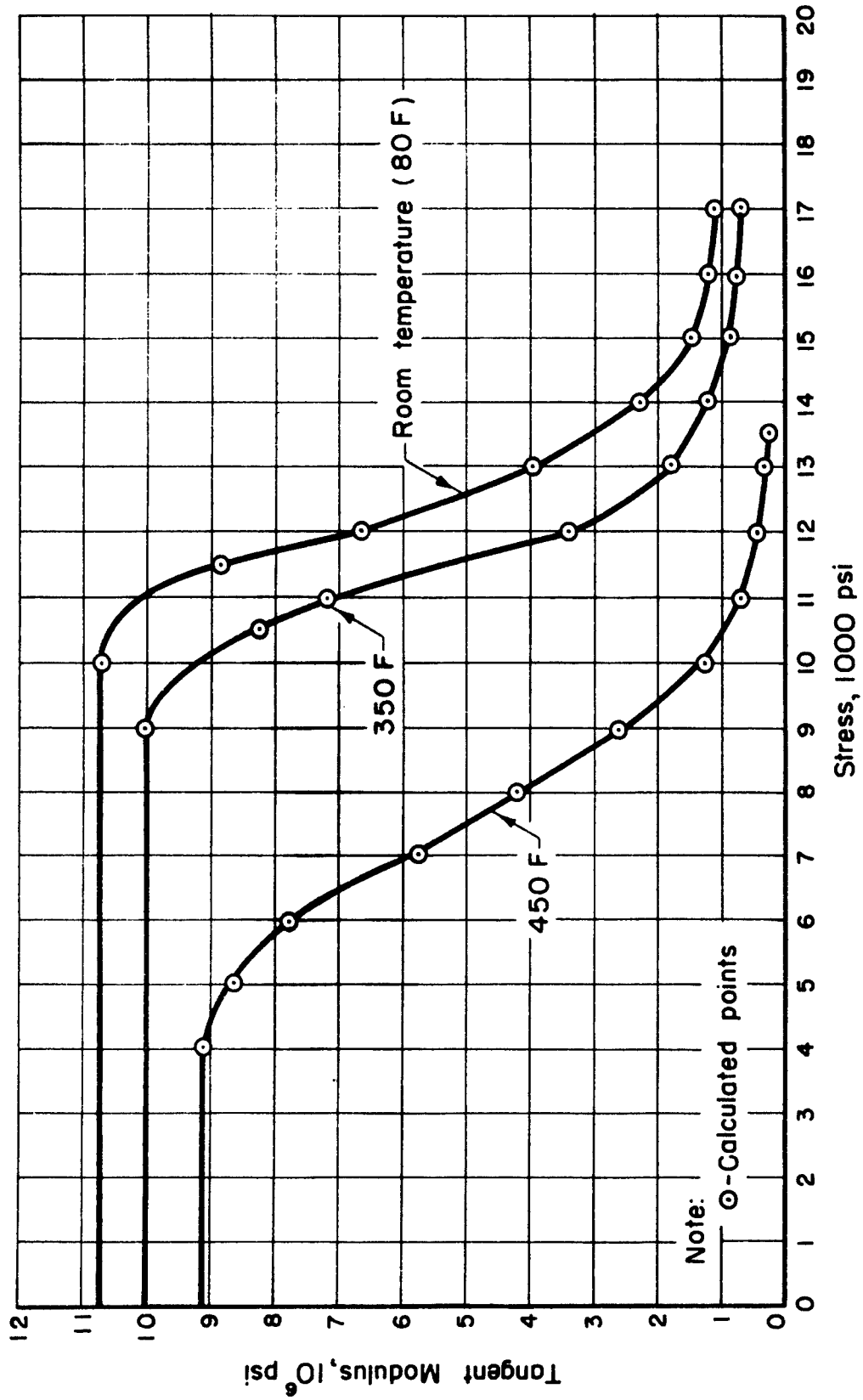


FIGURE 14. VARIATION OF TANGENT MODULUS WITH STRESS IN COMPRESSION

In order to compare the tensile- and compressive-creep behavior, tests were conducted for several stresses at a test temperature of 450 F. The compression specimen used for these tests was the one of rectangular cross section as described in the section on test specimens.

Four values of stress were used for these tests, and the results consistently indicated that the test material creep rate for a given stress level was considerably greater in compression than in tension during a 200-hour-test period. For example, for a stress of 9000 psi, the creep strain in compression was more than twice that for tension at a test time of 70 hours. Since these results appeared to be somewhat questionable, it was decided to run additional tests on a compression specimen of an alternative design. The design chosen was the one of circular cross section described in the section on test specimens. This specimen was somewhat larger than the previously used specimen, and it was felt that the possibility of having a gage section that was influenced by end effect was less likely.

Using the alternative compression specimen, additional compression creep tests were conducted at both 450 F and 350 F. For 450 F, the results of one compression specimen and one tension specimen tested at 7000 psi and one compression specimen and one tension specimen tested at 8000 psi are given in Figure 15. For the tension curves, each point shown is the average of two simultaneous strain readings. It will be noted, however, that the simultaneous readings which give the dashed average curve for each compression test have both been plotted. An averaging of these readings without a presentation of the individual test points was not justified, since the differences were large.

An additional tension-creep curve for a stress of 8250 psi has also been plotted in Figure 15. The plotted points shown are the average of two simultaneous strain readings.

At the test temperature of 350 F, one tension specimen and one compression specimen were tested at 9000 psi. The results of these tests are given in Figure 16 where the simultaneous readings for the compression test and the average of the simultaneous readings for the tension test have been plotted.

An additional tension-creep curve for a stress of 8000 psi at 350 F is plotted in Figure 16. The plotted points shown are the average of two simultaneous readings.

In the above test results, it will be noted that the simultaneous compression-creep readings were, in general, quite different in magnitude. This difference is a consequence of the fact that a slight initial misalignment usually becomes magnified with increasing compressive loading. In tension, of course, the specimen has a tendency to be self-aligning.

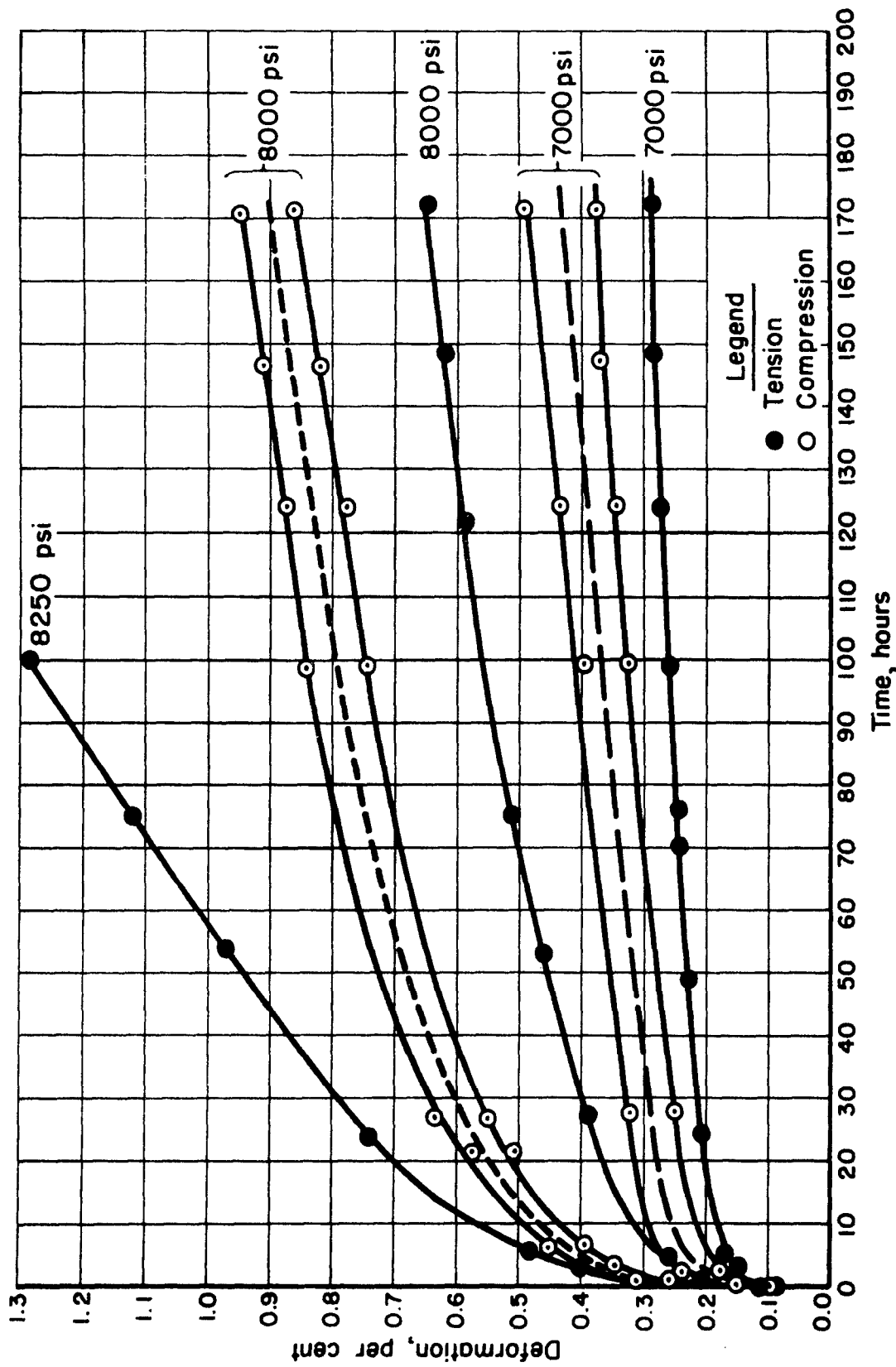


FIGURE 15. TENSION - AND COMPRESSION - CREEP CURVES FOR STABILIZED 24S-T4 ALUMINUM ALLOY TESTED AT 450 F

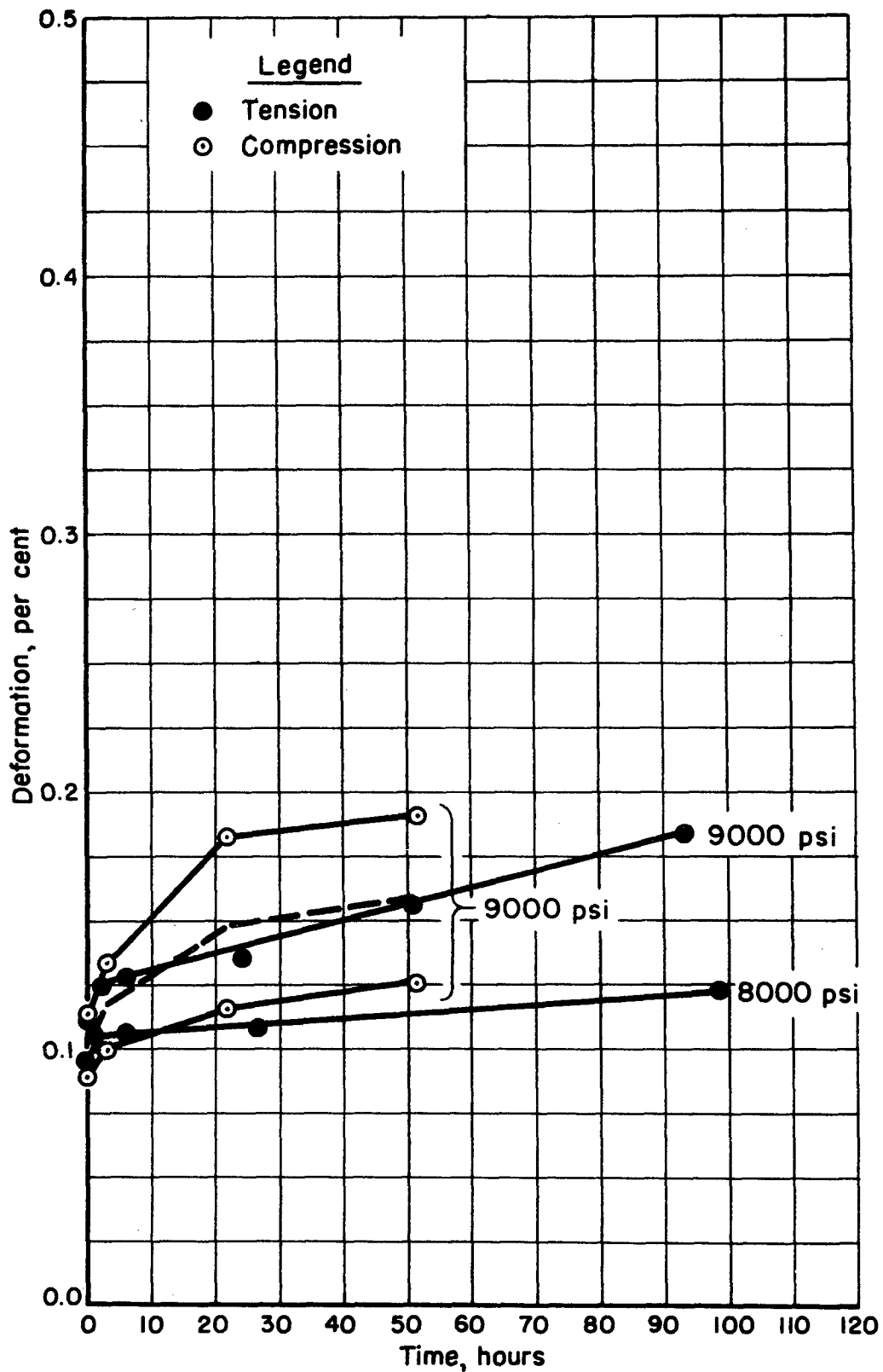


FIGURE 16. TENSION- AND COMPRESSION - CREEP CURVES FOR STABILIZED 24S-T4 ALUMINUM ALLOY TESTED AT 350 F

The test results presented in Figures 15 and 16 indicate, it is felt, that for stresses approximately equal to or less than those considered, the use of tension data in place of compression data would not introduce a serious error. In fact it is thought that the inherent difficulties of compression-creep testing are quite likely to produce results which are actually more in error than results obtained from tension-creep tests.

During the investigation, it was discovered that the range of stresses which were of interest in column creep extended to much lower values of stress than had been anticipated. For example, the initial stresses in the columns tested ranged from approximately 1000 psi to 7000 psi for the test temperature of 450 F, and from approximately 3000 psi to 10,000 psi for 350 F. Although the method of measuring strains used for the above results was satisfactory for the high ends of these stress ranges, it was not sufficiently sensitive for the lower values. As a consequence of this, it was necessary to introduce the use of a different method of strain measurement. The method selected utilized an electric capacitance-type gage, and was considerably more sensitive than the previously used strain gage. Tests using this method are being conducted at present, but the results have not yet progressed sufficiently to permit their presentation.

At the time the outline for the present investigation was prepared, it was planned to conduct column-creep tests at 300 F. For reasons which will be discussed later, this temperature was abandoned in favor of the temperature of 350 F. Before the change was made, however, some tension-creep tests were conducted at 300 F. The results of these tests are best described by the tabulation below, which compares the results obtained at 300 F with those obtained later at 350 F.

<u>Temperature,</u> <u>F</u>	<u>Stress,</u> <u>psi</u>	<u>Approximate Creep</u> <u>in 200 hours, %</u>
300	18,000	0.15
350	9,000	0.16

From this tabulation, it can be seen that the resistance to creep at 300 F is considerably greater than at 350 F.

### Column Tests

#### Room Temperature

Room-temperature, immediate-failure tests were conducted in order to obtain a relative idea of the loss in column-load capacity due to temperature.

Tests were conducted in accordance with the outline given in the section on test procedures with the exception that loading was continued to failure. The results of the room-temperature column tests are given in the tabulation below:

<u>L/r</u>	<u>Approx. Failure Load, pounds</u>	<u>Estimated Effective Eccentricity, inches</u>
156	423	0.0095
106	768	0.0060
56.5	1330	--

The estimated effective eccentricity was obtained by means of a Southwell plot of the test data. (7) This method makes use of the fact that the column load-deflection equation can be arranged in the form of a relation involving the variables, deflection,  $\delta$ , and deflection over load,  $\delta/P$ . The relation involving these variables is linear and the  $\delta$  axis intercept gives the value of the effective eccentricity (as defined in the Test Procedures section). The eccentricity for the column with  $L/r = 56.5$  was not estimated because the deflections caused by elastic loads were too small for an accurate estimate.

### 300 F

At the beginning of the investigation, it was intended to conduct column-creep tests at 300 F. After a few tests, it was concluded that column-creep data could not be obtained at 300 F.

For a column with  $L/r = 156$ , a load of 416 pounds was used, and although failure did occur after 90 hours, the deflection-time curve was a staircase-type function in which large, abrupt deflections were followed by periods in which relatively little deflection took place. An explanation of this behavior was based upon the fact that the experimentally determined immediate-failure load for this column at 300 F was approximately 430 pounds. Since the load of 416 pounds was very close to the immediate-failure load, the column was quite sensitive to slight external disturbances, and the failure at the end of 90 hours was the result of a series of disturbances.

Further references to the behavior of the test columns at the temperature of 300 F will be found in later sections of this report.

### 350 F

According to the test procedure described for column tests, the test columns were to be adjusted to a value of  $C = L/1200$  at room temperature, and then tested at 350 F. An examination of the load-deflection

data at the test temperature, however, revealed that the value of  $C$  increased slightly due to the temperature rise. The best average value of  $C$  for all test columns except those with  $L/r = 56.5$  was found to be approximately  $L/1080$ . For these columns the values were within the range of  $C = L/1140$  and  $C = L/1010$ . The value of  $C$  for  $L/r = 56.5$  could not be determined accurately, because the loading caused inelastic deformation before appreciable deflection took place.

A calculation for the above columns reveals that the change in length and cross section due to thermal expansion could not cause the change in  $C$  that was observed. It can only be concluded that the column configuration, that is, the initial curvature and eccentricity of load application, changed.

The results of the immediate-failure tests at 350 F are given in the tabulation below:

<u>L/r</u>	<u>Approx. Failure Load, pounds</u>
156	420
131	610
106	791
81.4	1030
56.5	1270

For the column-creep tests, an attempt was made to cover a range of failure times from approximately 1/2 hour to 200 hours. The results of these tests for the test temperature of 350 F are presented in Figures 17 through 21 as a family of curves of total deflection (deflection due to load) versus time with load as the parameter. The variation of the experimental points from the curves as shown was a maximum of about  $\pm 3 \times 10^{-3}$  inch for some parts of the long-time tests on the columns with  $L/r = 156$  and 131. For the remaining curves, the variation was less than  $\pm 2 \times 10^{-3}$  inch.

Further remarks regarding the characteristic shape of these curves will be deferred until later in the report.

#### 450 F

According to the test procedure described for column tests, the test columns were to be adjusted to a value of  $C = L/1200$  at room temperature, and then tested at 450 F. An examination of the load-deflection data, however, revealed that the value of  $C$  increased due to the rise in temperature. The best average value of  $C$  for all test columns except those with  $L/r = 56.5$  was found to be approximately  $L/900$ . For these columns the values were within the range given by  $C = L/960$  and  $L/850$ .

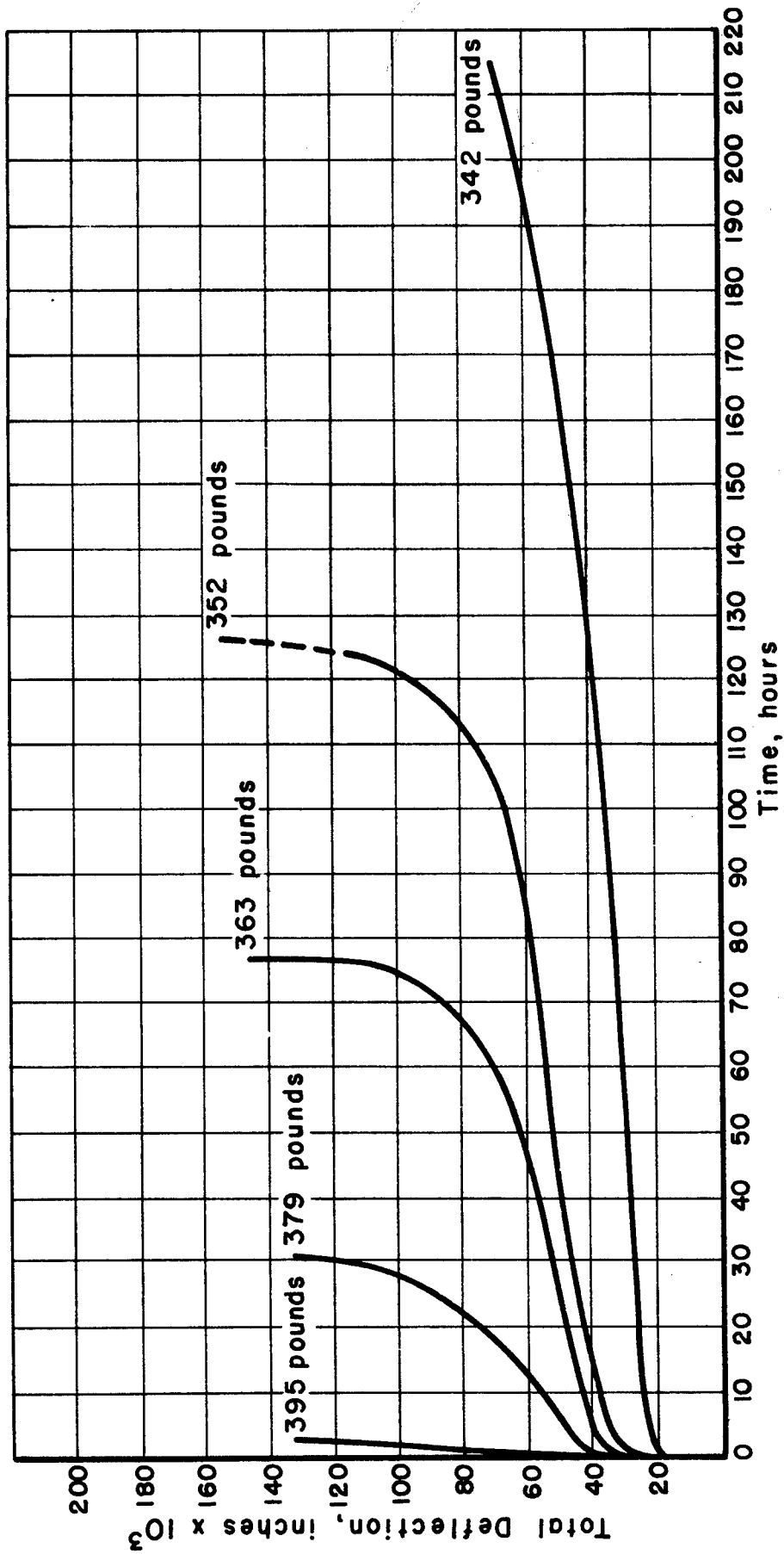


FIGURE 17. TOTAL DEFLECTION-TIME CURVES FOR STABILIZED 24S-T4 ALUMINUM-ALLOY COLUMNS WITH  $\frac{L}{r} = 156$ , TESTED AT 350 F

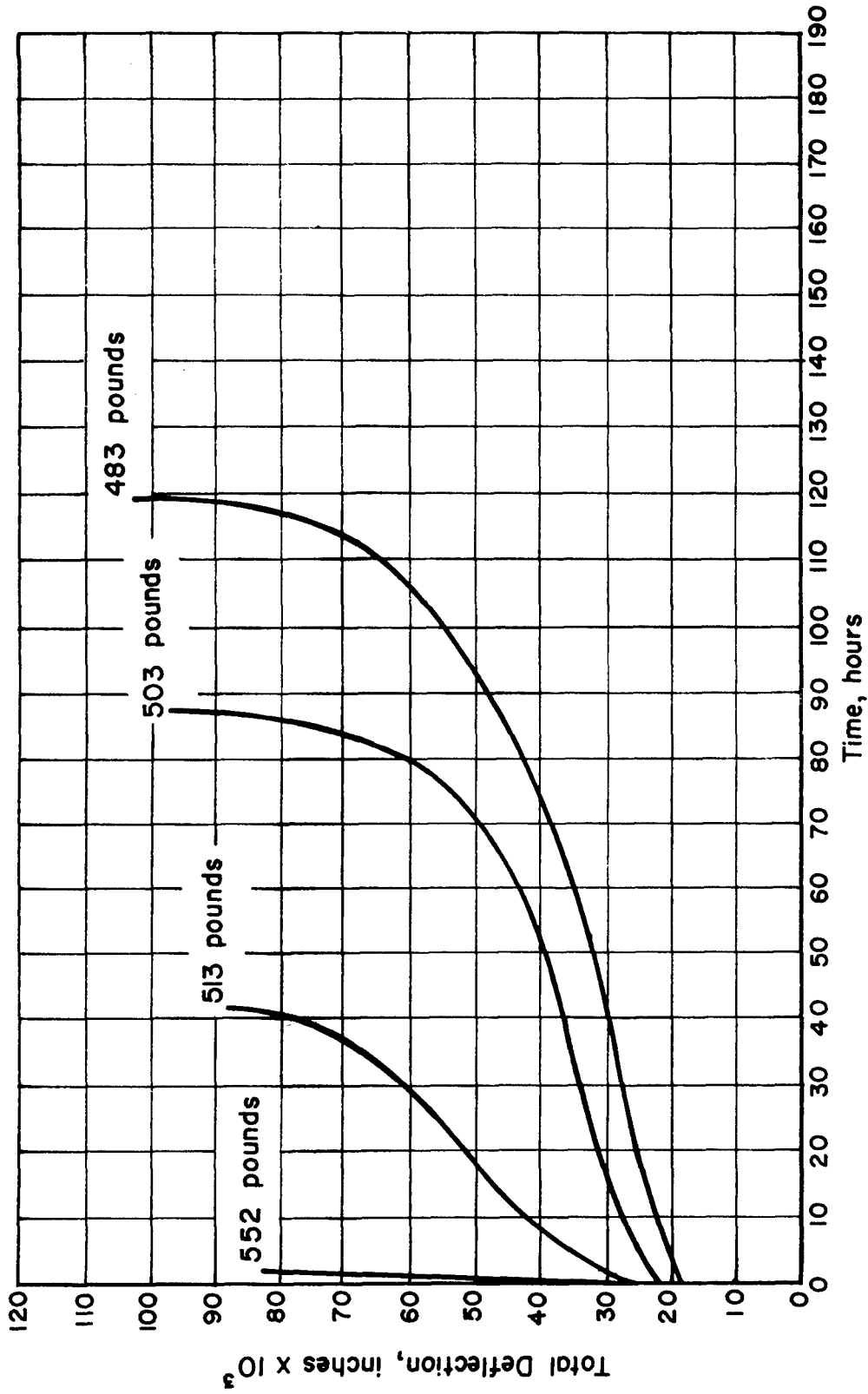


FIGURE 18. TOTAL DEFLECTION-TIME CURVES FOR STABILIZED 24S-T4 ALUMINUM-ALLOY COLUMNS WITH  $\frac{L}{r} = 131$ , TESTED AT 350 F

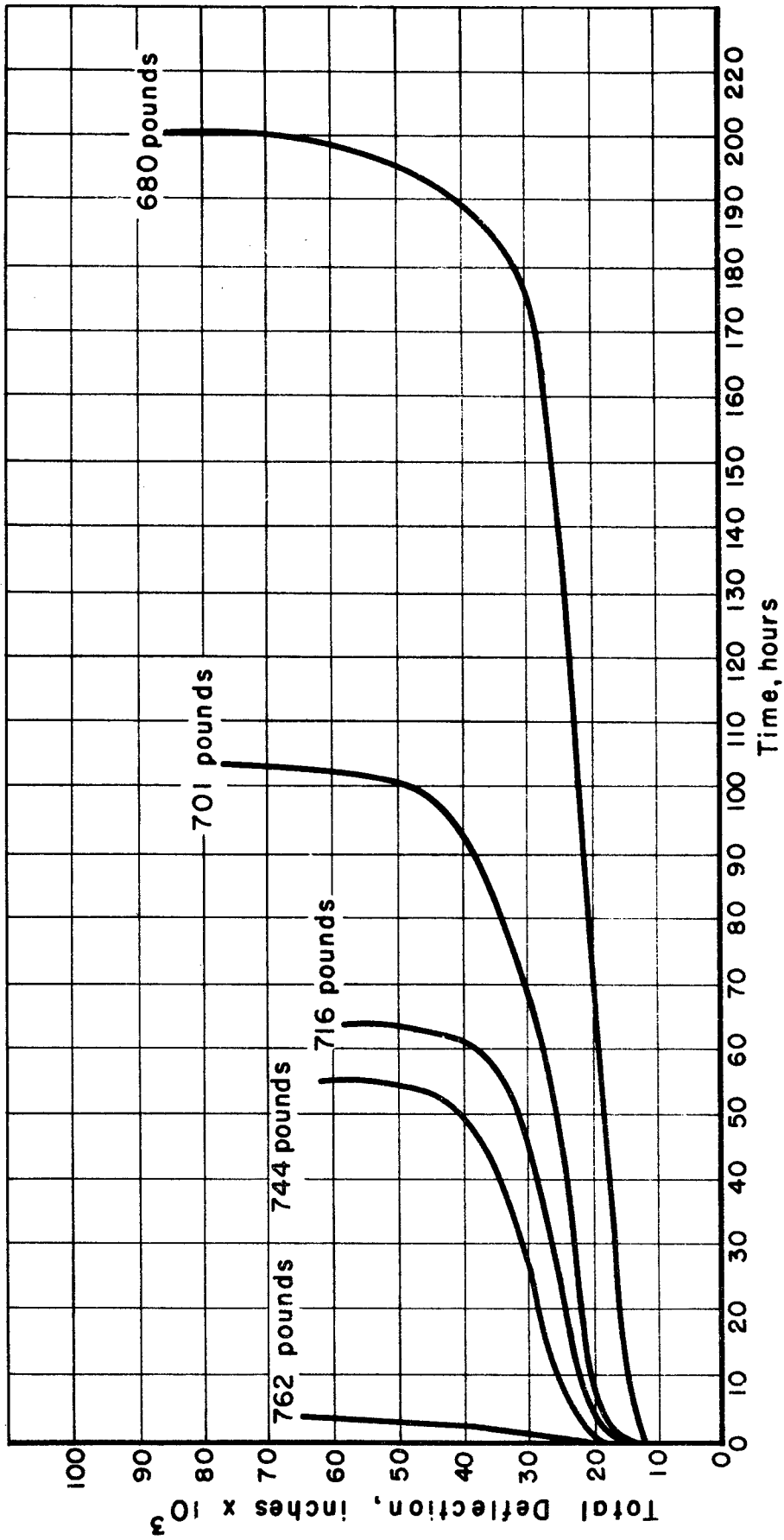


FIGURE 19. TOTAL DEFLECTION-TIME CURVES FOR STABILIZED 24S-T4 ALUMINUM-ALLOY COLUMNS WITH  $\frac{L}{r} = 106$ , TESTED AT 350 F

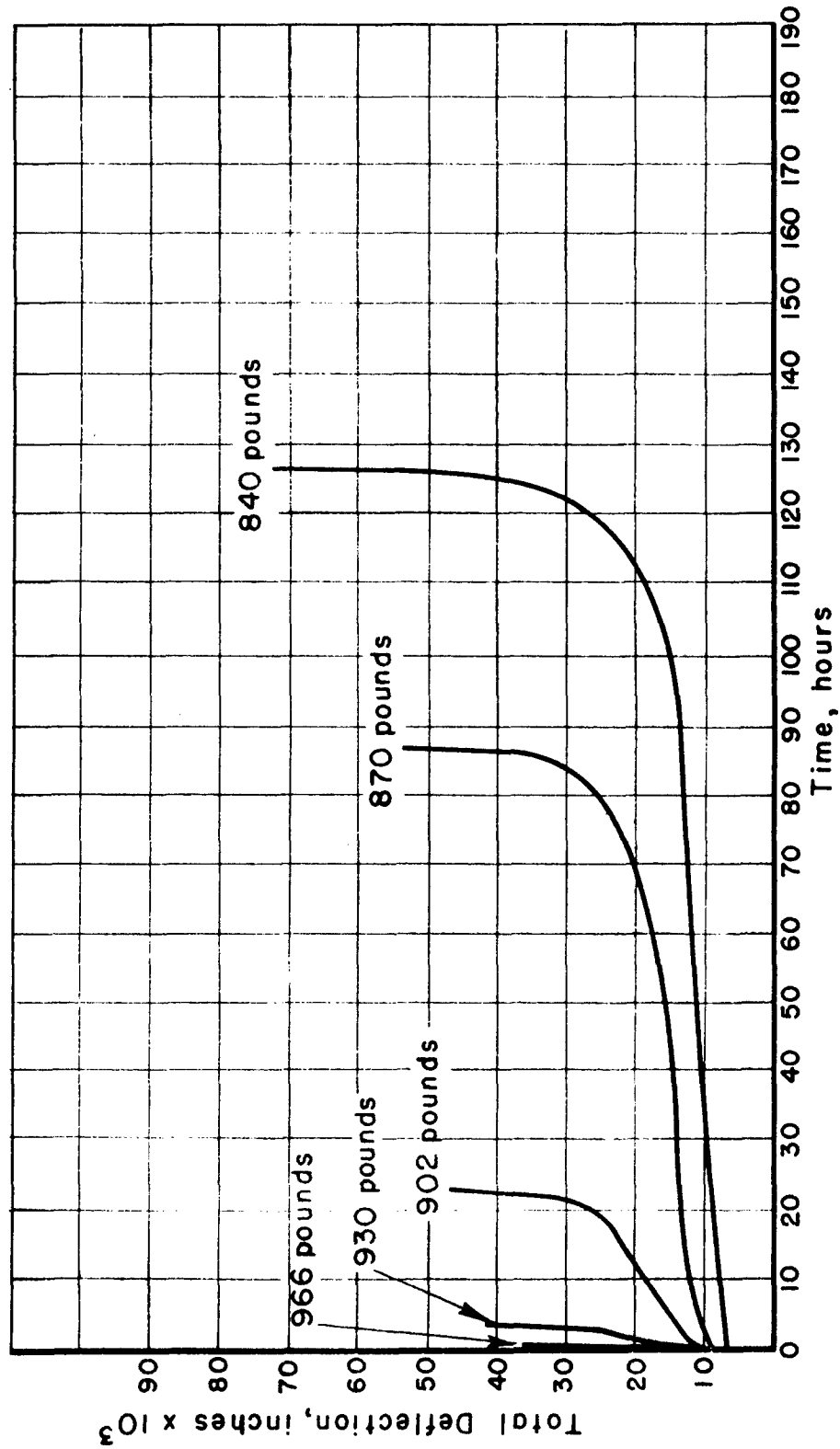


FIGURE 20. TOTAL DEFLECTION-TIME CURVES FOR STABILIZED 24S-T4 ALU-MINUM-ALLOY COLUMNS WITH  $\frac{L}{r} = 81.4$ , TESTED AT 350 F

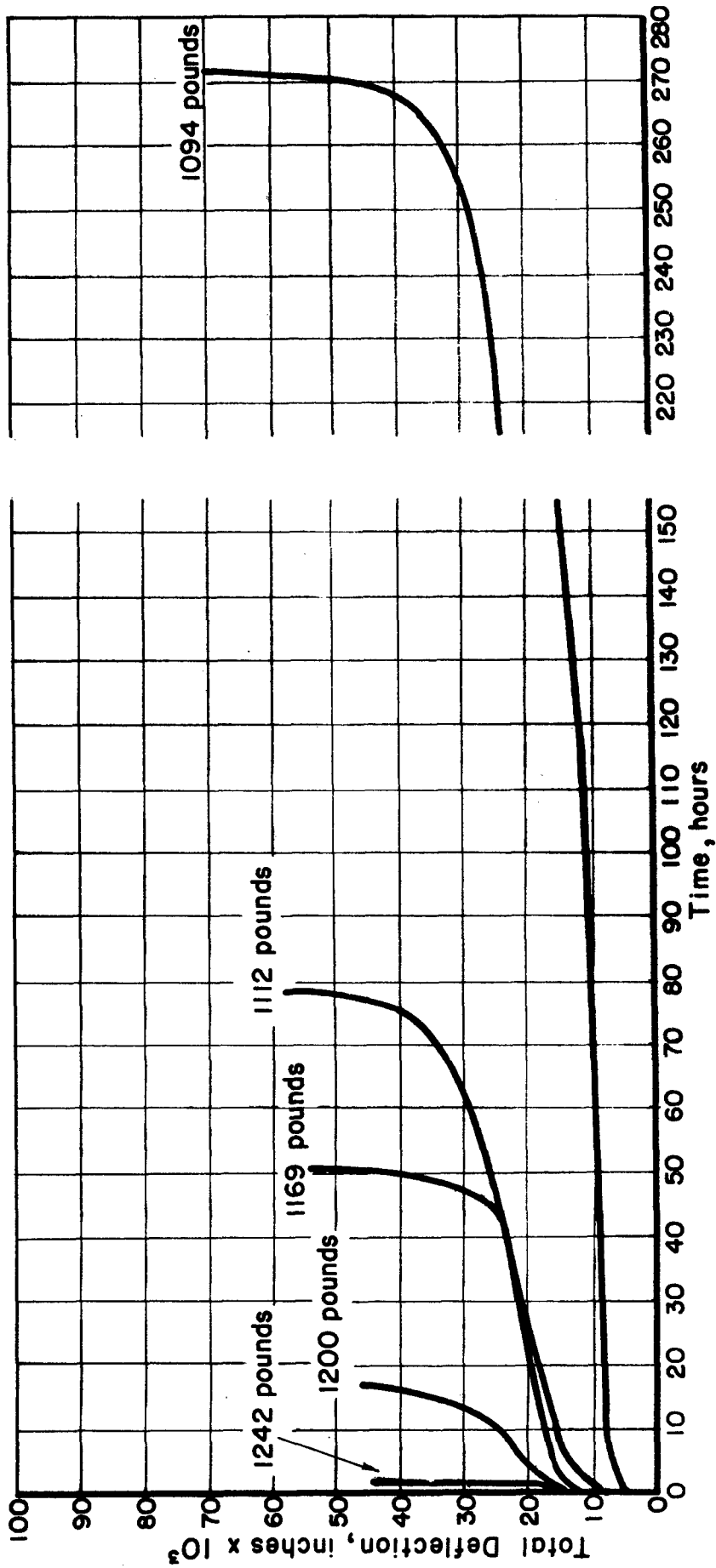


FIGURE 21. TOTAL DEFLECTION - TIME CURVES FOR STABILIZED 24S-T-4 ALUMINUM-ALLOY COLUMNS WITH  $\frac{L}{r} = 56.5$ , TESTED AT 350 F

The results of the immediate-failure tests at 450 F are given in the tabulation below:

<u>L/r</u>	<u>Approx. Failure Load, pounds</u>
156	374
131	458
106	567
81.4	721
56.5	967

For the column-creep tests, an attempt was made to cover a range of failure times from approximately 1/2 hour to 200 hours. The results of these tests for the test temperature of 450 F are presented in Figures 22 through 26 as a family of curves of total deflection (deflection due to load) versus time with load as the parameter. The variation of the experimental points from the curves as shown was a maximum of  $\pm 3 \times 10^{-3}$  inch for parts of the long-time tests on columns with  $L/r = 156$  and 131. For the remaining curves, the variation was less than  $\pm 2 \times 10^{-3}$  inch.

## GENERAL DISCUSSION OF COLUMN CREEP

### The Creep Behavior of Perfect Columns

Although the behavior of perfectly straight, axially loaded columns subject to creep may not appear to be of practical value, a brief discussion of the conditions necessary for instability is of interest because it does provide a basis for a general discussion.

A detailed discussion of the conditions necessary for instability is given in Appendix I. The essential results of this discussion, however, will be given in this section.

If a perfect column is loaded to a value of load  $P$  which is less than the value of load  $P_T$  given by the tangent modulus load, it will be stable in the straight form. If creep takes place, it will be a uniform compressive creep. Whether or not the given column will become unstable depends upon whether or not the stress-strain properties of the material are affected by the creep which has taken place. If the tangent modulus of the stress-strain curve at the stress level given decreases with time due to creep, it is possible that conditions will eventually exist for instability in the straight form.

Since the load in the considered case is constant with time, the criterion for instability will be given by a reduced- or double-modulus-type

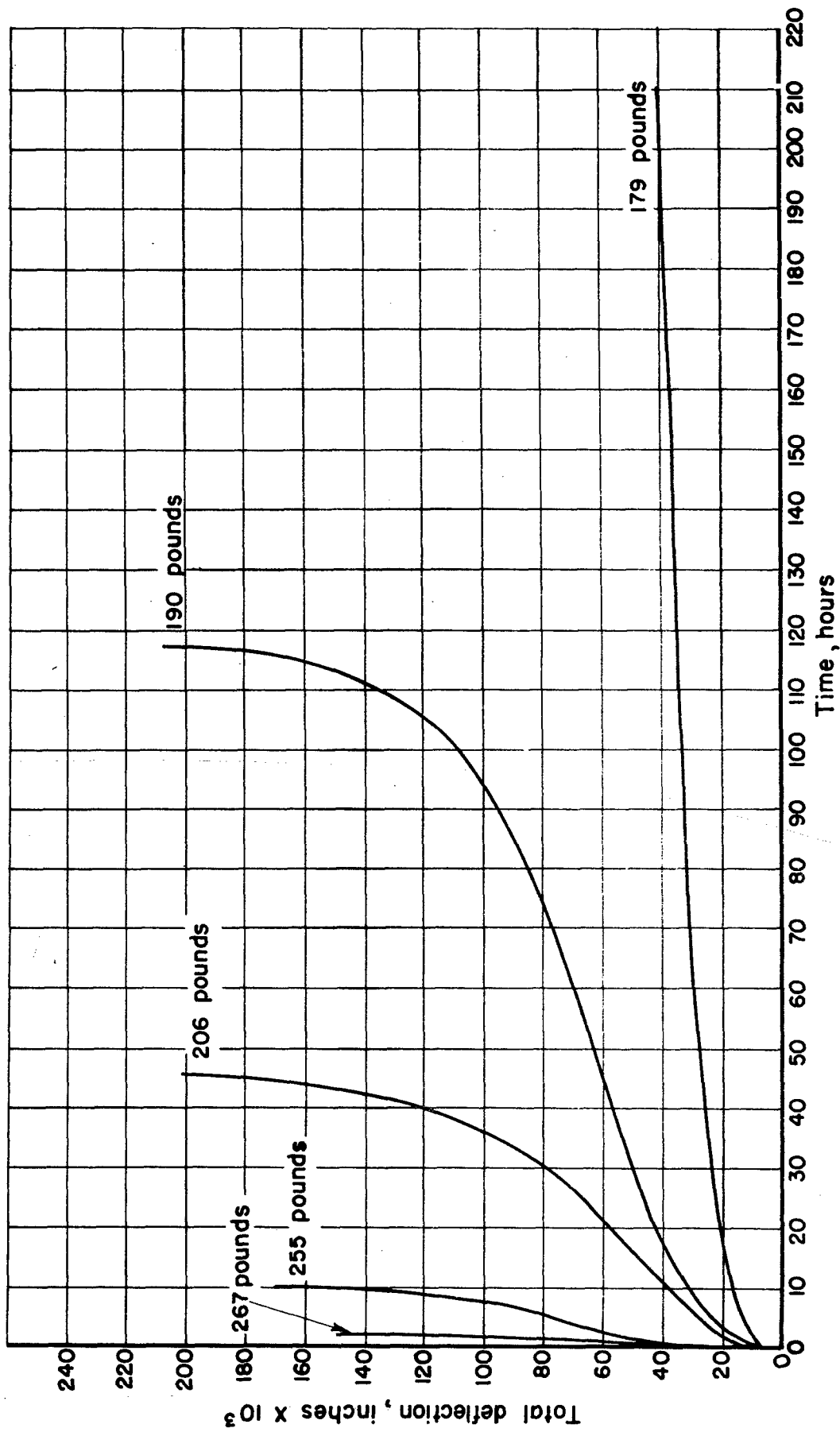


FIGURE 22. TOTAL DEFLECTION-TIME CURVES FOR STABILIZED 24S-T4 ALUMINUM-ALLOY COLUMNS WITH  $\frac{L}{r} = 156$ , TESTED AT 450F

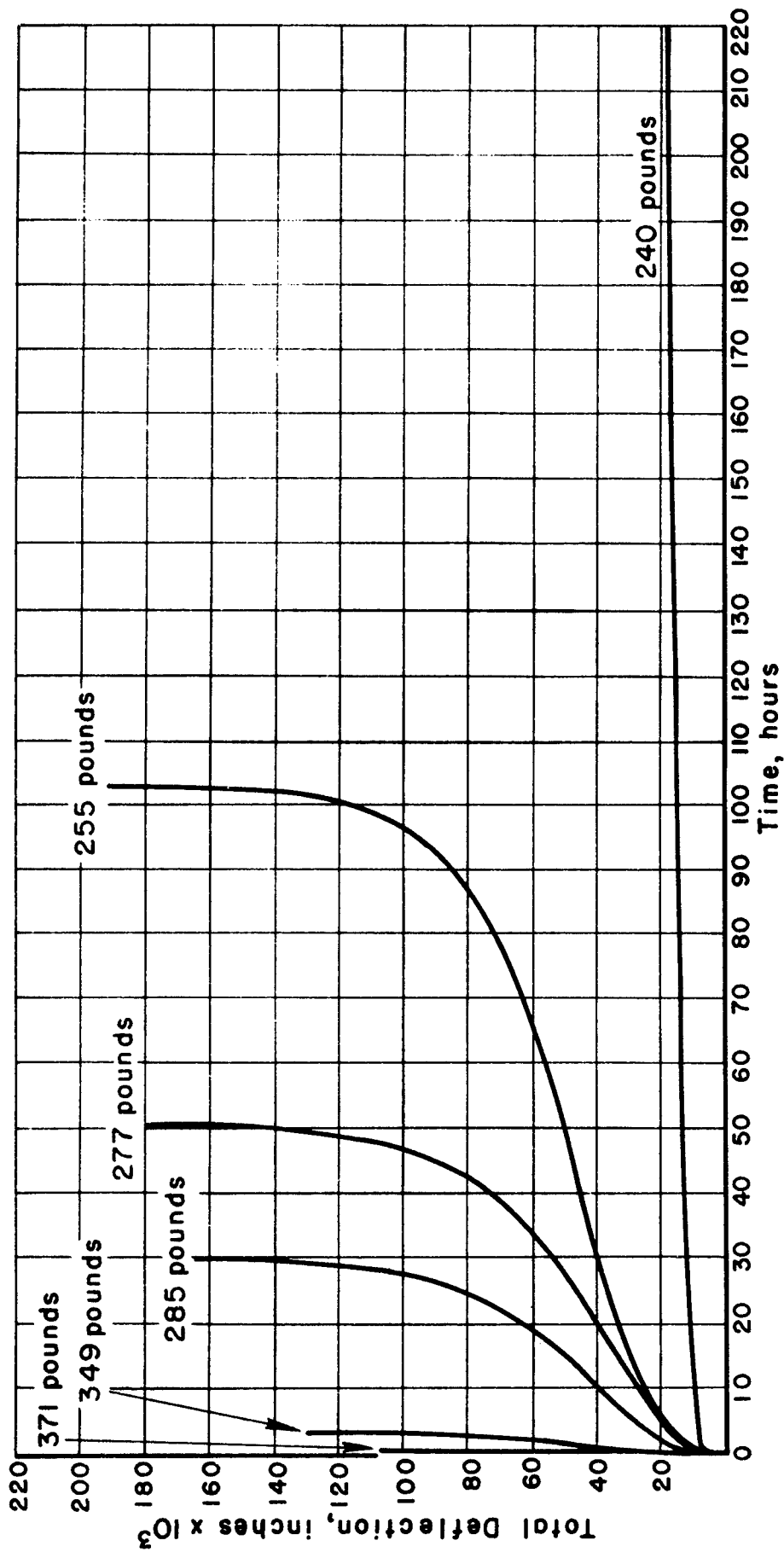


FIGURE 23. TOTAL DEFLECTION-TIME CURVES FOR STABILIZED 24S-T4 ALUMINUM-ALLOY COLUMNS WITH  $\frac{L}{r} = 131$ , TESTED AT 450F

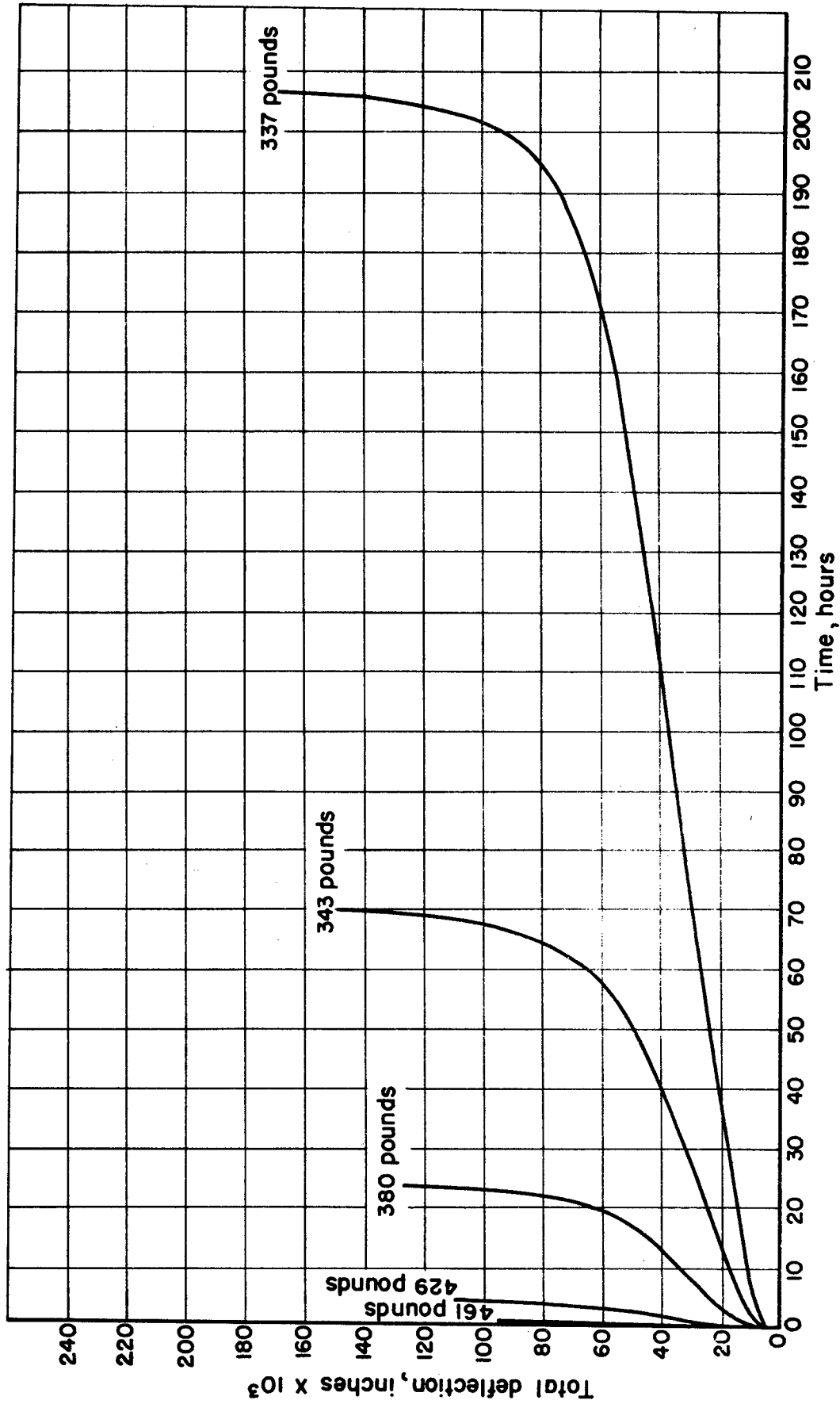


FIGURE 24. TOTAL DEFLECTION-TIME CURVES FOR STABILIZED 24S-T4 ALUMINUM-ALLOY COLUMNS WITH  $\frac{L}{r} = 106$ , TESTED AT 450F

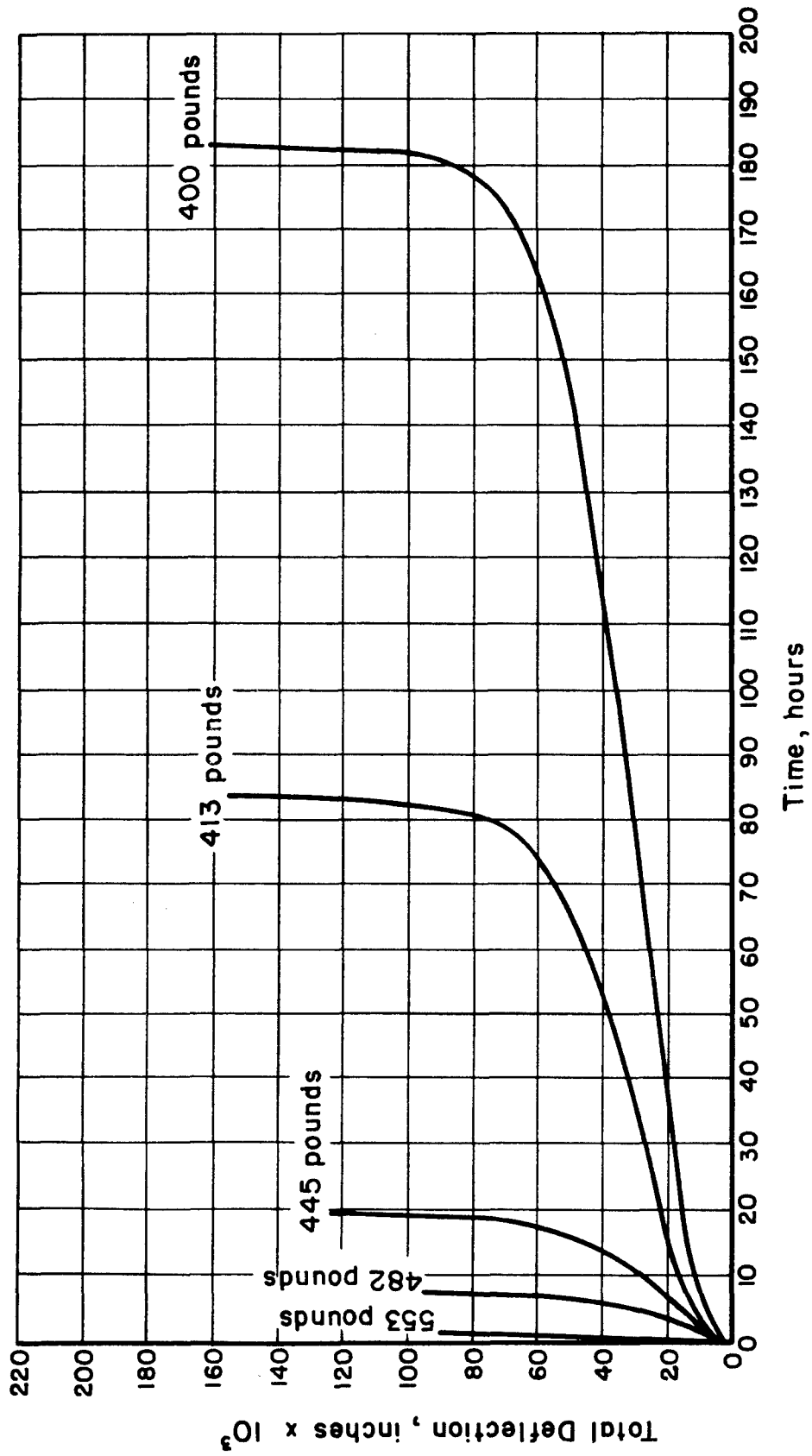


FIGURE 25. TOTAL DEFLECTION - TIME CURVES FOR STABILIZED 24S-T4 ALUMINUM-ALLOY COLUMNS WITH  $\frac{L}{r} = 81.4$ , TESTED AT 450 F

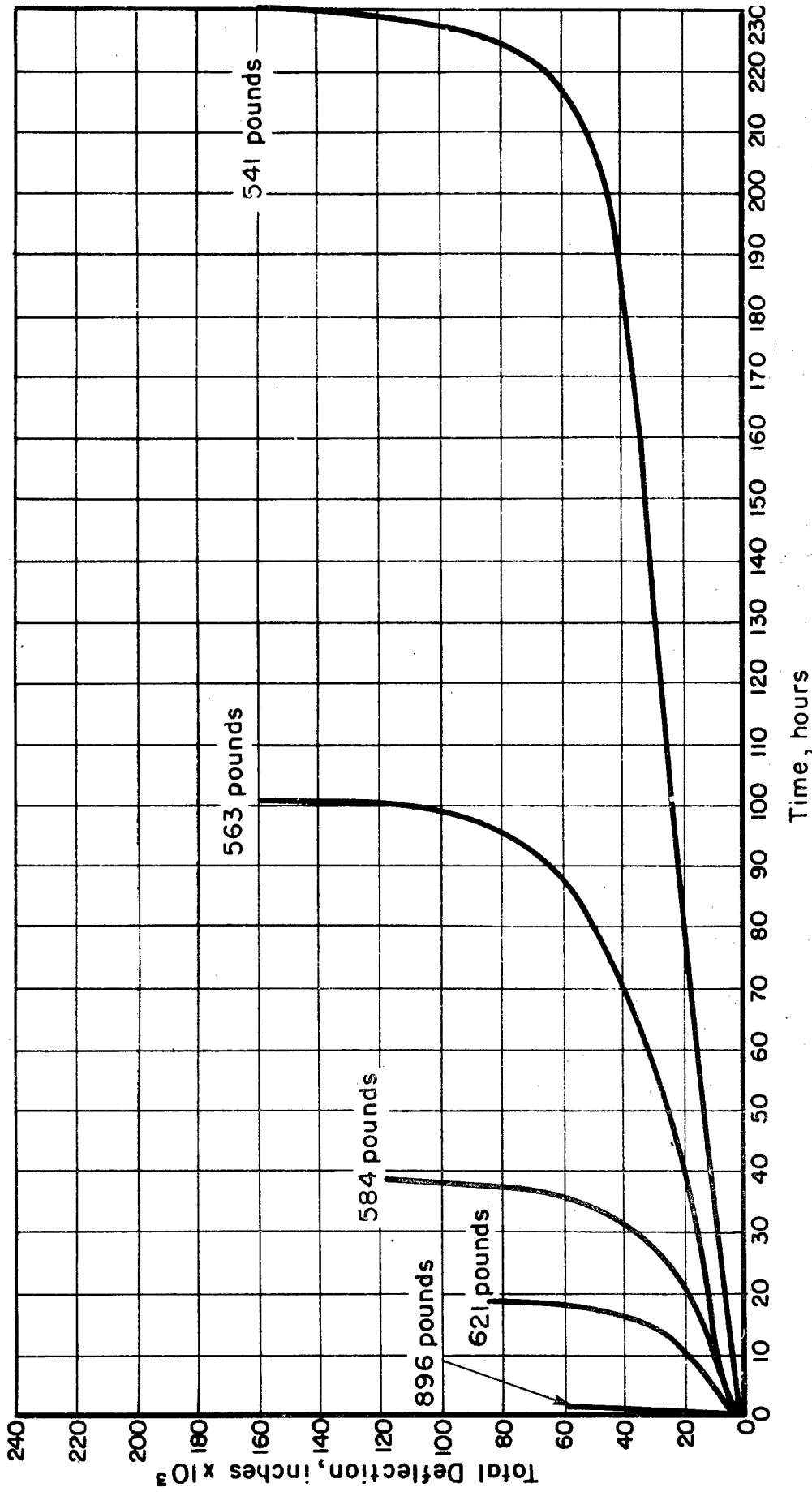


FIGURE 26. TOTAL DEFLECTION-TIME CURVES FOR STABILIZED 24S-T4 ALUMINUM-ALLOY COLUMNS WITH  $\bar{T} = 56.5$ , TESTED AT 450 F

consideration. The so-called tangent-modulus-type consideration would not be valid since in such a consideration, bending of the column must proceed simultaneously with increasing axial load.

In the above stability consideration, creep was responsible for the stress-strain property change necessary to produce instability in the straight form of the column. Another mechanism which could cause instability in time is a metallurgical change in the column material. If the material stress-strain curve became lower with time, the curve giving the criterion for instability would also become lower with time. In time, then, it is conceivable that a column which was safe initially might become unstable due to the metallurgical changes that have occurred. A consideration of this type would become important whenever a column is subjected to temperatures sufficiently high to cause such metallurgical changes.

### The Creep Behavior of Imperfect Columns

An ideal treatment of the column problem in which creep is considered would be based upon a solution which would yield, for a given load, the column configuration at any time. It follows, of course, that the time for failure or collapse would be the end result of such a solution, and it might then seem that the designer could make use of such a solution in the design of structures which need only last for a short, known length of time.

Unfortunately, a general solution of the above type does not exist at present. It is of interest to note, however, that, even if such a solution did exist, design based on a short expected life would probably prove to be a hazardous proposition. This would be true since such factors as load, load eccentricity, column curvature, end fixity, possible overloads, and temperature conditions can at best be only approximately estimated in most structures. An inaccurate estimate of any one of these factors could easily prove to be disastrous.

During the period covered by this report, some thought was devoted to the development of a method which would, first, describe in as simple a manner as possible the column action during creep, and second, possibly be of value as an approximate solution for long-time tests.

The method eventually developed, and presented in this report as Appendix II, is an extension of Popov's method which was formulated to describe the creep behavior of a beam subjected to pure bending.

According to the method introduced, the column configuration at the end of a time,  $t$ , is determined by considering the changes in deflection occurring during small intervals of time, and summing the results to the desired time. During each small, time interval, the deflection change is a consequence of the creep strains and elastic adjustment strains that occur during the interval. The determination of the value of the creep strains

that take place is given by the stress level at the point considered, and the length of the time interval (for each interval, the stress causing creep at a point is considered constant, hence, the time interval must be small). The elastic adjustments are selected in such a manner as to assure that plane column cross sections remain plane, and that the internal and external force and moment balance is maintained. From the preceding discussion, it can be seen that the method described would be best adapted to cases in which the deflection velocity is small. In such cases, the time intervals chosen would not prove so likely to be impractically small.

In the method introduced in Appendix II, the only requirement regarding load was that the load produce an initial stress distribution which is elastic throughout. Since this requirement was achieved experimentally on some columns that were in the short range, the method would be usable during at least the initial part of some short-column creep calculations.

As was mentioned earlier, the use of the method outlined could best be applied to the solution of long-time tests in which the deflection rate was small. Fortunately, it was found that the experimentally determined load versus failure-time curves in the vicinity of 200 hours gave large increases in failure time for small decreases in load. It appeared that for each column, there was a load below which the column would not collapse due to creep. According to this type of behavior, the allowable load for a given column would be that maximum load which produces an initial stress distribution which will give a transient-type deflection versus time curve.

In order to determine this stress distribution, it would only be necessary to investigate the column behavior from the time  $t = 0$  to a short time beyond. A calculation of this type should be possible with the method outlined. Calculations are not yet possible, however, as an expression for creep in the low-stress, microinch-strain range is not available.

It should be noted that all of the remarks in this section refer to a temperature-stabilized material, such as the one used in this investigation. The change in properties accompanying metallurgical transformations could, of course, be expected to complicate the above conclusions.

#### Use of Test Results

In order to make use of the column test results presented earlier in the report, it is necessary to establish what constitutes a column-creep failure. It will be remembered that the typical column-deflection versus time curve was a curve for which the deflection velocity decreased with time up to an inflection point at which the rate of change of deflection velocity was zero. After the inflection point, the deflection velocity increased with time until the column could no longer support its load. Although the time at which the inflection point occurs may be considered in a sense the failure time, this time will not be designated as the failure time since the column can and

does support its load beyond this time. As a consequence, that time at which collapse occurs will be designated as the failure time in the presentation that follows.

Through the use of the curves of Figures 17 through 26, curves of the type shown in Figures 27 and 28 have been derived. In these figures, the plotted points give the failure time for the column loads used.

It will be noted that for the curves of each test temperature, there appears to be a lower limit below which failure due to creep will not occur. Since the load versus failure-time curves for the short columns level off at values of load above the loads which cause failures in the longer columns, it can only be concluded that, though creep will occur in the short columns at loads below its so-called lower limit, an adjustment occurs which enables the column to support its load without deflecting to failure.

The possibility of such an adjustment for a given column would, of course, be subject to the initial eccentricity present. The smaller the initial eccentricity, the more gradual will be the stress gradient across the column cross section. The more gradual the stress gradient is, the more likely the possibility that an adjustment will occur.

Making use of the curves of Figures 27 and 28, the curves of Figures 29 and 30 have been obtained. In each of these figures, the curves for immediate failure, and failure in 5, 50, and 200 hours have been plotted. The immediate failure values are those which were reported earlier in the section on test results. It should be pointed out that true immediate-failure tests at the test temperatures was not possible. This stems from the fact that during loading, column creep began at values of load below the immediate-failure load. Since the loads could not be applied abruptly, the deflection which occurred due to creep naturally affected the final load possible.

It will be noted that the plotted curves do not include the values for  $L/r = 56.5$ . The reason for this is that the sharp upward trend of these points reflects the fact that the value of  $C$  for  $L/r = 56.5$  was evidently less than the value of  $C$  stated for the remaining columns. The difficulties encountered in the estimation of  $C$  for the column with  $L/r = 56.5$  were discussed in the section on test results.

For purposes of comparison, the tangent-modulus and double-modulus theory curves have been plotted for both test temperatures. In spite of the imperfection present in the tested columns, it can be seen that their resulting curves have retained the characteristic shape of the perfect column curves. It should be noted that the stress levels attained by the experimental points are determined by the degree of imperfection (eccentricity) present. For columns with less imperfection, the points would, of course, be higher.

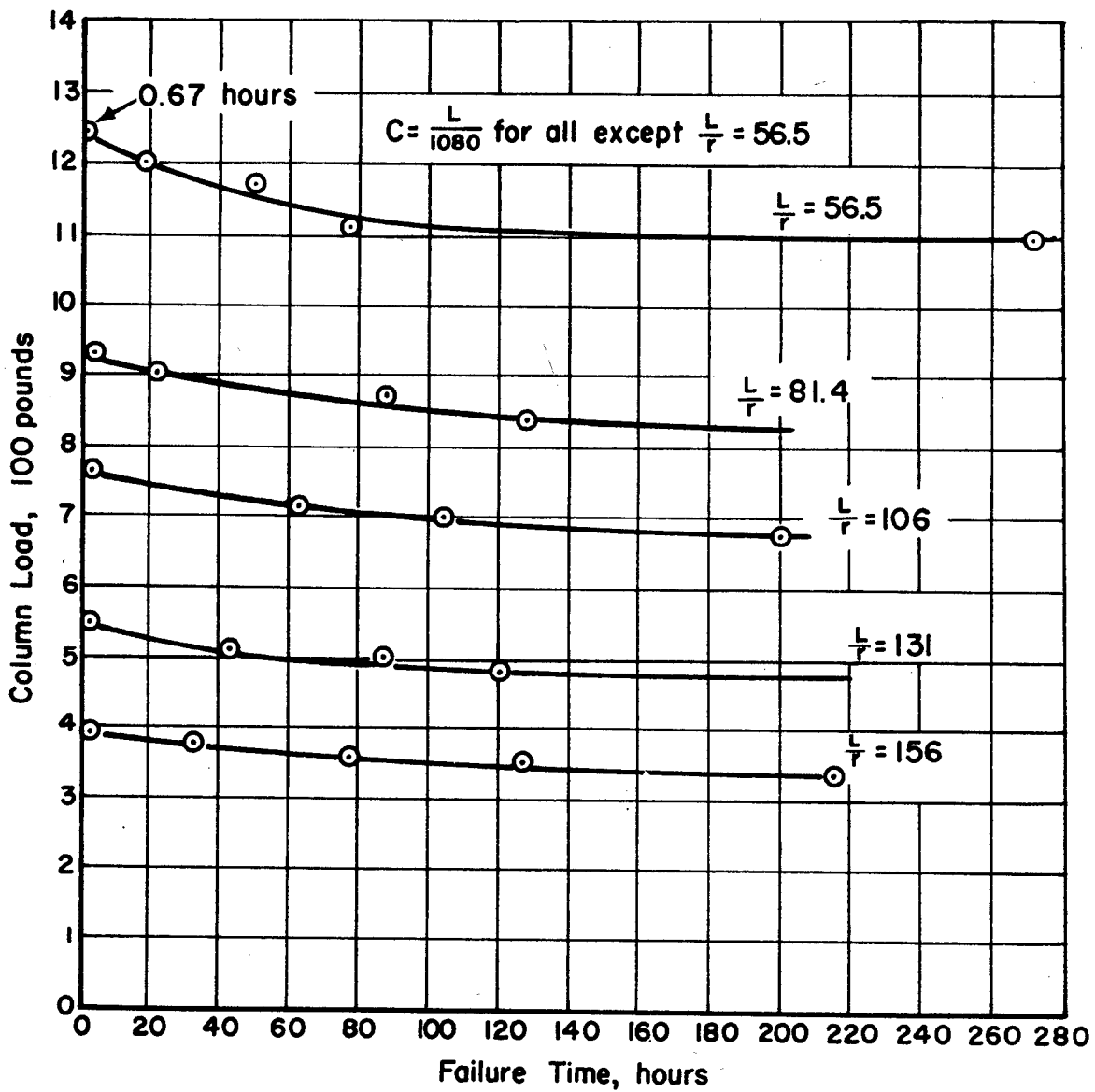


FIGURE 27. COLUMN LOAD VERSUS FAILURE TIME AT TEST TEMPERATURE OF 350 F

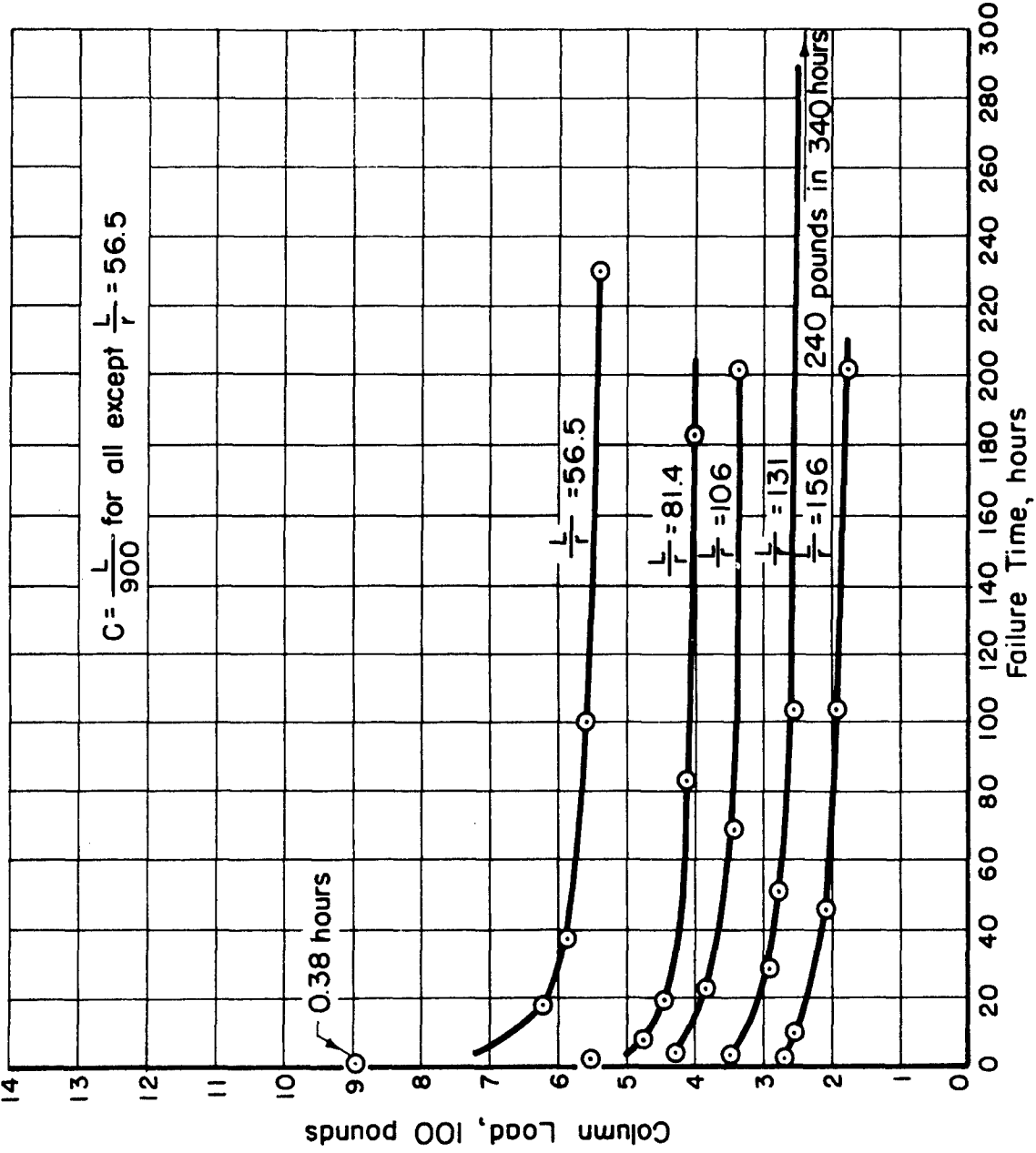


FIGURE 28. COLUMN LOAD VERSUS FAILURE TIME AT TEST TEMPERATURE OF 450 F

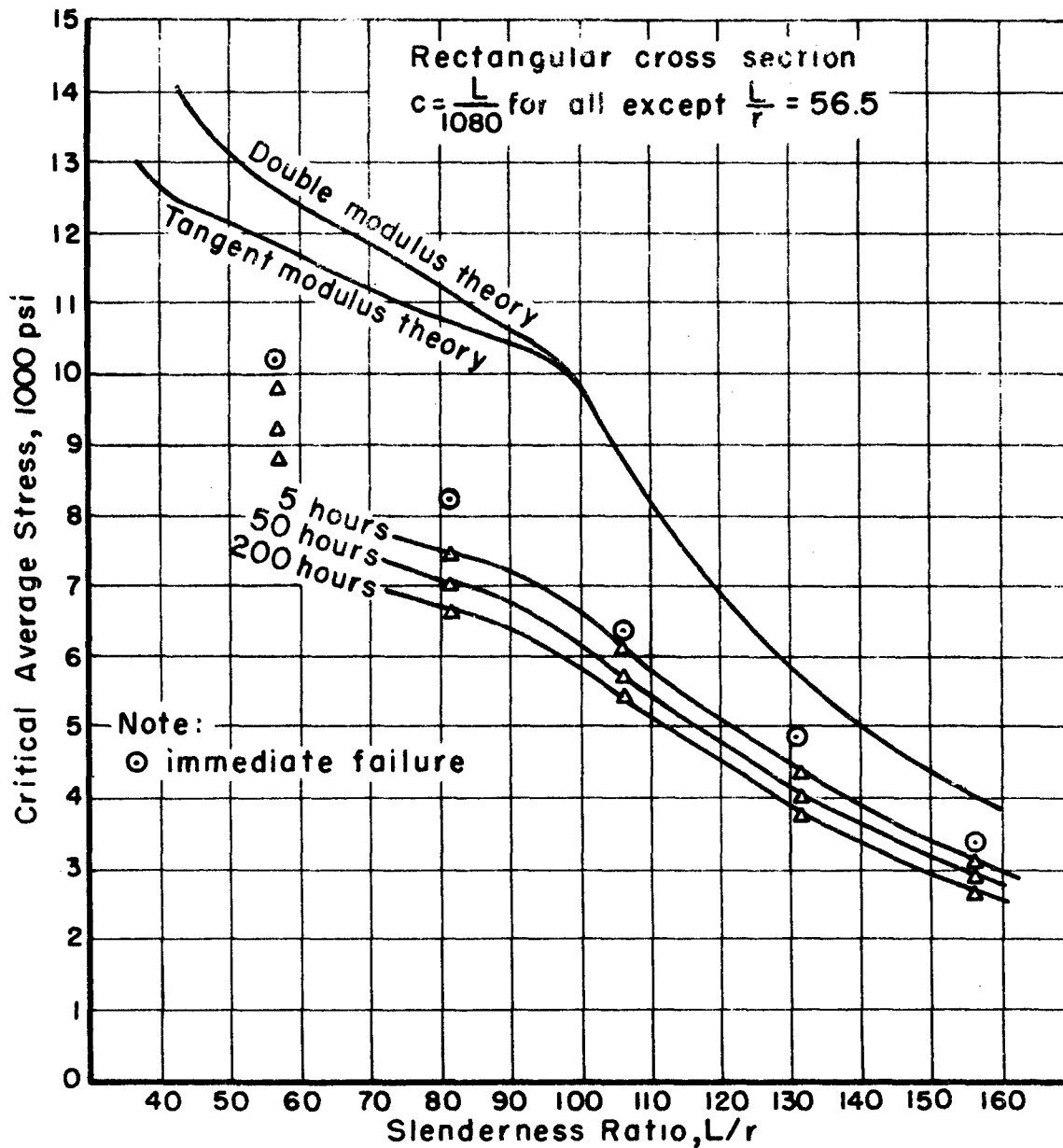


FIGURE 29. CRITICAL AVERAGE STRESS VERSUS SLENDERNESS RATIO WITH FAILURE TIME AS A PARAMETER AT TEST TEMPERATURE OF 350 F

A - 3341

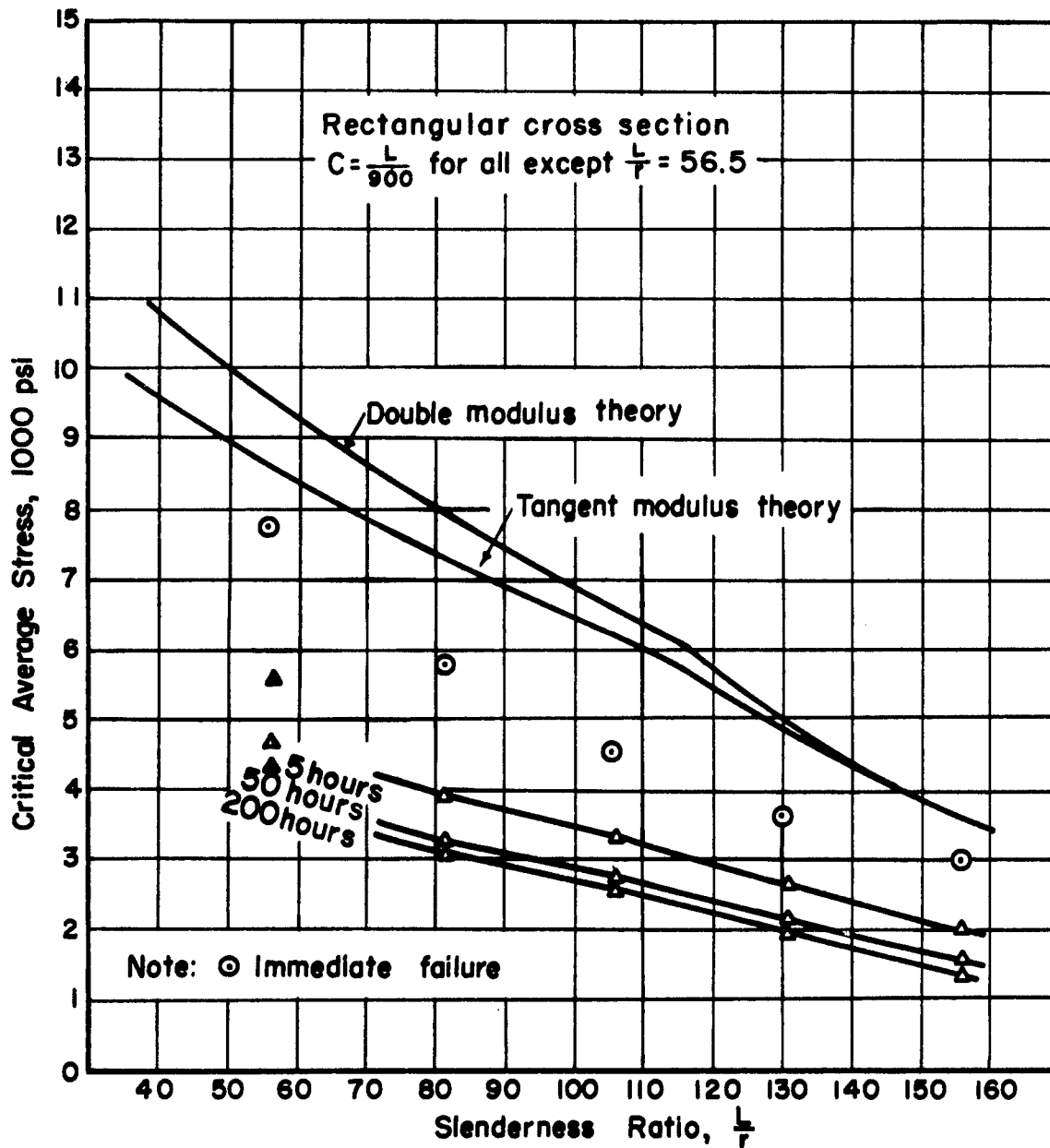


FIGURE 30. CRITICAL AVERAGE STRESS VERSUS SLENDERNESS RATIO WITH FAILURE TIME AS A PARAMETER AT TEST TEMPERATURE OF 450 F

One of the interesting trends to be noted from the curves of Figures 29 and 30 is that for a given column, the difference in load between an immediate failure load and a 200-hour failure load decreases with decreasing temperature. In order to illustrate this point, the tabulation below is given:

<u>Temperature,</u> F	<u>*Difference for</u> L/r = 156, psi	<u>*Difference for</u> L/r = 81.4, psi
450	1600	2600
350	650	1600

\*Difference between average stress for immediate failure and 200-hour failure.

From this trend, it might be predicated that the above difference will tend to zero with decreasing temperature. As will be remembered, the column-test results at the temperature of 300 F indicated that this was the case. It can be concluded then that below a certain temperature immediate failure will occur before stresses sufficiently high to cause creep failure are attained.

One of the more important aspects of these curves from a design point of view is that they illustrate forcibly the possible danger of column design based on immediate-failure loads. This is particularly true for the test temperature of 450 F. For this temperature, the load at 200 hours is approximately half that for immediate failure.

As another means of illustrating the effect of temperature on the load-carrying capacity of the test columns, a plot of average stress versus L/r for all the test temperatures is given in Figure 31. For the room-temperature curve, the immediate-failure values have been plotted. For 350 F and 450 F, the 200-hour failure curves have been plotted, since it is felt that these most nearly represent the limiting load which the columns can support. (It should be noted that in the L/r range of the 200-hour curves the initial stress distributions were elastic throughout.) As can be seen from these curves, the separation between the 350 F and the 450 F curves is much greater than the separation between the 350 F and room-temperature curves. It is of interest to note that this large increase in sensitivity to temperature between 350 F and 450 F can also be detected in the yield-strength versus temperature curve of Figure 12.

From a consideration of the curves of Figures 12 and 31, it would appear that a limitation of the use of the test material in columns to temperatures below approximately 400 F might be wise, since the load-carrying capacity can be expected to drop rapidly above 400 F. For temperatures above 400 F, it would seem that more efficient design could be accomplished by the use of a more temperature-resistant alloy.

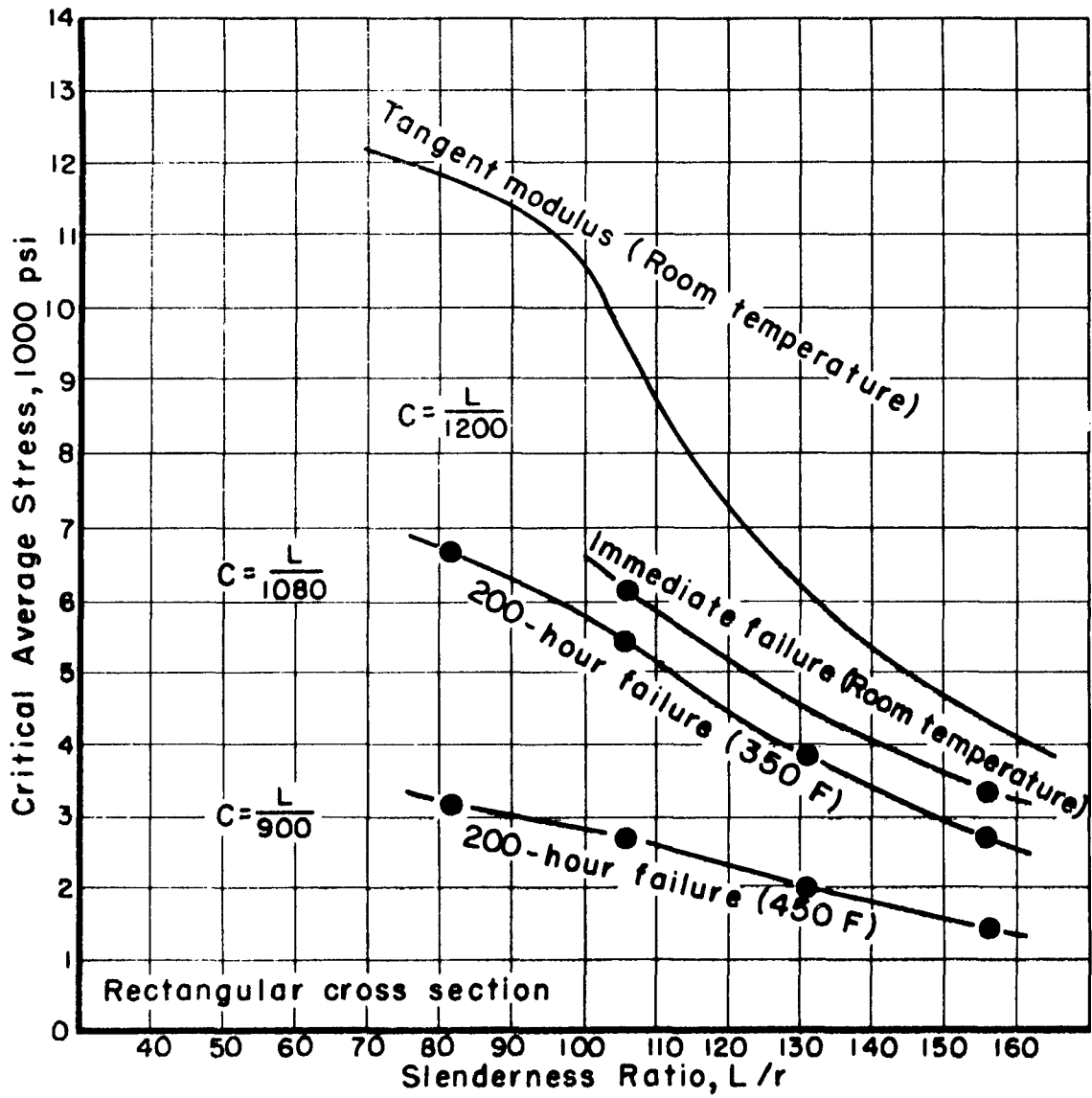


FIGURE 31. CRITICAL AVERAGE STRESS VERSUS SLENDERNESS RATIO FOR THREE TESTING TEMPERATURES

## Design Considerations

One of the first problems that arises in the design of columns for use at elevated temperatures is that of determining the temperature at which time-dependent deformation (creep) becomes important. In this investigation, it was found that for columns of 24S-T4 (stabilized) aluminum at a test temperature of 300 F, immediate-failure loads could be reached before stresses sufficiently high to cause "buckling creep" were produced. From this behavior, it can be concluded that for temperatures up to approximately 300 F, procedures used for room-temperature column design would be satisfactory. (The mechanical property values used should, of course, be for the temperature considered.)

One indication that creep need not be considered at 300 F was given by the fact that the stress necessary to cause measurable creep in simple tension was found to be considerably higher than that which could be expected on the basis of column calculations. This creep behavior at 300 F was described in the section of this report on test results.

It is felt that another indication of the critical temperature range for column creep can be seen in the variation of yield strength with temperature. It was found in the test results that the value of yield strength decreased slowly with increasing temperature up to approximately 300 F. After 300 F, the decrease was much more rapid.

It should be noted, of course, that these observations refer to a temperature-stabilized material. The use of the above indications as a basis for design of columns of unstabilized material would not be justified. A brief mention of the stability problems involved in columns of unstabilized material was made earlier in this report in the general discussion of column creep.

As was emphasized previously, column-design calculations involving creep should be based on a consideration which determines the maximum load that a column can support, and still have a transient-type deflection versus time curve. Since this calculation is not possible as yet, an alternative method will be introduced. It is based upon the probable fact that if a transient-type deflection curve is to be achieved, the stress levels at the convex and concave faces of the column must produce not only a transient-type creep, but also initial creep rates which cannot be too different in magnitude. Since it would be expected that elastic stresses are most likely to produce these conditions, the limitation placed on the maximum stress in the column cross section should be that it not exceed a certain elastic stress. For purposes of this discussion, the limiting stress chosen is the proportional limit of the material at the test temperature.

In equation form, this states that

$$\sigma_{p.L.} = \frac{P}{A} + \frac{Pyh}{2I}$$

where  $\sigma_{p.L.}$  is the proportional limit,

P is the column load,

A is the cross-section area,

y is the deflection at the mid-point,

h is the depth of the column cross section,

I is the moment of inertia about the bending axis.

The deflection, y, is

$$y = \frac{C}{1 - L^2 \frac{P}{\pi^2 EI}}$$

where E is Young's modulus at the test temperature, and L is the column length.

A plot of this equation for the two test temperatures is given in Figure 32. Since the 200-hour-failure loads most nearly represent the limiting load, they have been plotted in the figure. It will be noted that although the agreement is fairly good for the lower L/r ratios, the experimental points tend to diverge from the curve for higher L/r ratios. Although an empirical adjustment which makes the allowable maximum stress a function of the slenderness ratio could be made to improve the agreement in the longer range, it is felt that it would be preferable to specify an upper limit on the slenderness ratios that are used. For the columns used in this investigation, it would appear that a value of about  $L/r \approx 110$  would prove satisfactory.

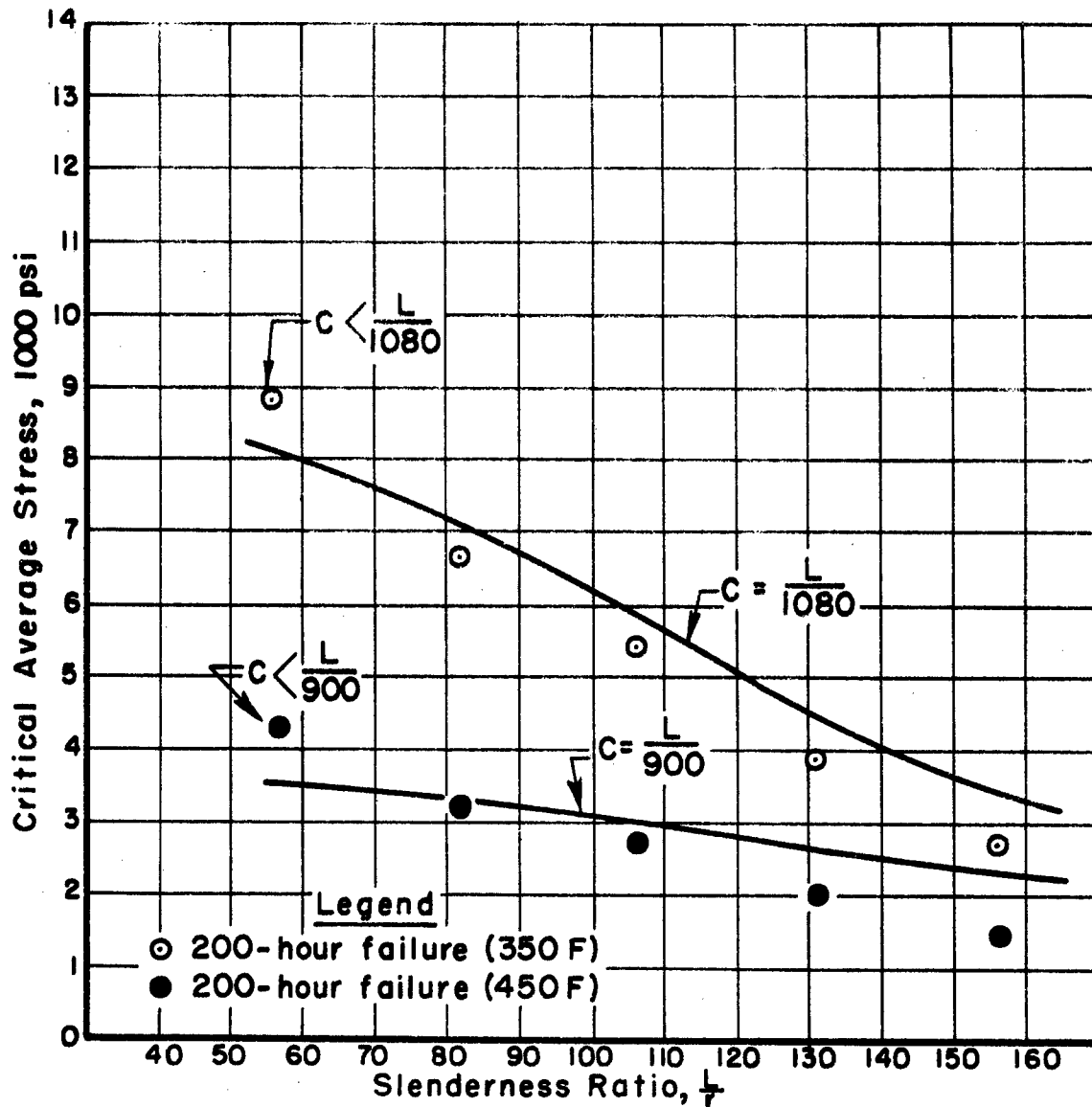


FIGURE 32. COMPARISON OF LIMITING AVERAGE STRESS CURVES AND EXPERIMENTAL RESULTS

## REFERENCES

1. Higgins, T. P., "Effect of Creep on Column Deflection", The Rand Corporation, P-51, December 1, 1948.
2. Libove, Charles, "Creep Buckling of Columns", Institute of Aeronautical Science, Preprint No. 353, January, 1952.
3. Rosenthal, D., and Baer, H. W., "Creep Buckling of Columns", Publication of the Department of Engineering, University of California, Los Angeles, California.
4. Day, Emmett, "Characteristics of Electric Strain Gages at Elevated Temperatures", Proceedings of the Society for Experimental Stress Analysis, Volume IX, No. 1, 1951.
5. Popov, E. P., "Bending of Beams With Creep", Journal of Applied Physics, March, 1949.
6. Roberts, Irving, American Society of Testing Materials, Preprint No. 37, 1951.
7. Timoshenko, S., Theory of Elastic Stability, McGraw-Hill Book Company, Inc., New York, 1952.
8. Shanley, F. R., "Analysis of Stress-Strain-Time Relations From the Engineering Viewpoint", The Rand Corporation, P-68, March 4, 1949.
9. Shanley, F. R., "Inelastic Column Theory", Journal of the Aeronautical Sciences, May, 1947.
10. Bleich, F., Buckling Strength of Metal Structures, McGraw-Hill Book Company, Inc., New York, 1952.

## APPENDIX I

### The Creep Behavior of Perfect Columns

During the past few years, considerable thought has been devoted to the problem of the behavior of imperfect columns subject to creep. Since the behavior of perfectly straight, axially loaded columns subject to creep has been neglected, it is felt that a brief discussion of the problem is worth while.

As a background for this discussion, the equations valid for ordinary theory of perfect columns will be listed, since it is felt that they can be utilized in the considerations to follow.

For elastic or slender columns, the critical average stress is given by the Euler formula

$$\sigma = \frac{\pi^2 E}{(L/r)^2} ,$$

where  $E$  is Young's modulus, and  $L/r$  is the column-slenderness ratio.

For short inelastic columns, the upper limit of the critical average stress is

$$\sigma = \frac{\pi^2 E_r}{(L/r)^2} ,$$

where  $E_r$  is the reduced or double modulus. The lower limit of the critical average stress is

$$\sigma = \frac{\pi^2 E_t}{(L/r)^2} ,$$

where  $E_t$  is the tangent modulus.

The theory which gives rise to these equations does not consider time or the effects of creep. It is, therefore, of interest to speculate as to the nature of the creep behavior of perfect columns.

Suppose that a column whose slenderness ratio is given by the Point O in Figure 33 is considered. If this column is loaded as indicated by the solid vertical line, it will become susceptible to bending at the Point A. If, however, the loading is stopped at the Point B, it will be stable in the straight form at the stress level given by the elevation of B above O.

Another manner of illustrating these loadings is given in Figure 34. The Point A' of Figure 34 corresponds to the Point A of Figure 33. This

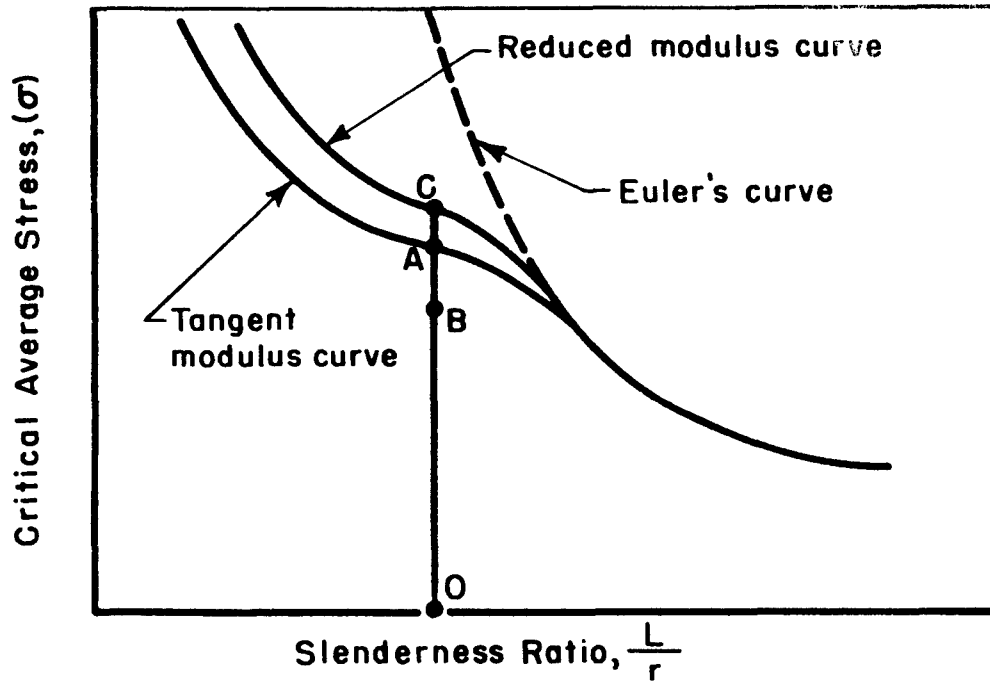


FIGURE 33. LOADING PROCEDURE ON A CRITICAL AVERAGE STRESS VERSUS SLENDERNESS RATIO DIAGRAM

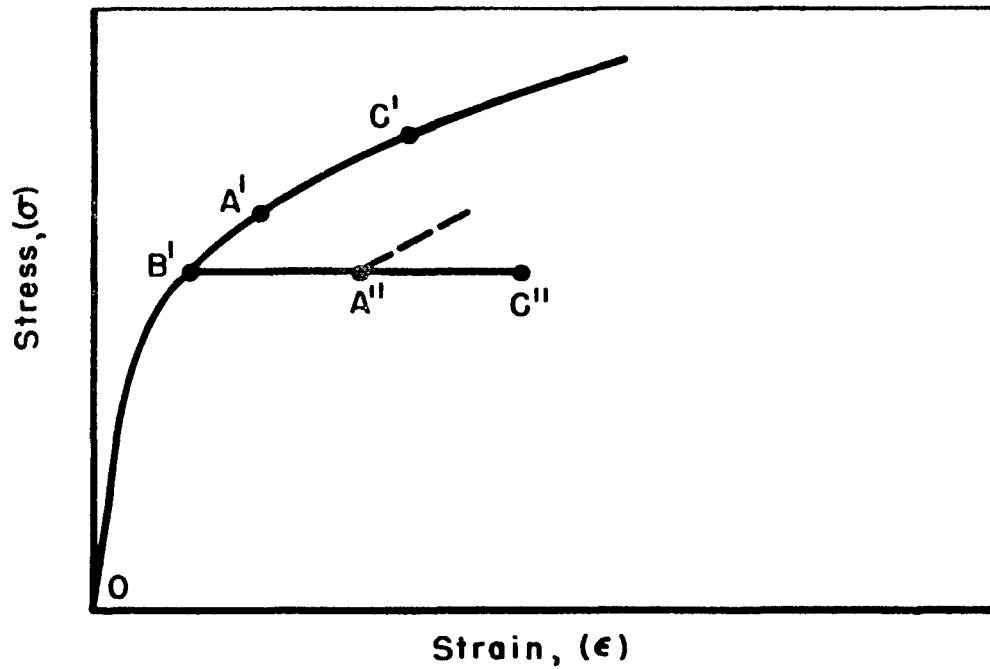


FIGURE 34. LOADING PROCEDURE ON A STRESS VERSUS STRAIN DIAGRAM

merely means that the ratio

$$\frac{\sigma(A')}{E_t(A')}$$

equals

$$\frac{\pi^2}{(L/r)^2}$$

at the Point A. In a similar manner, a Point C', where

$$\frac{\sigma(C')}{E_r(C')}$$

equals

$$\frac{\pi^2}{(L/r)^2}$$

will correspond to Point C. For the Point B of Figure 33, there will correspond a point such as B' of Figure 34. For the Point B', the value of

$$\frac{\sigma(B')}{E_t(B')}$$

is less than

$$\frac{\pi^2}{(L/r)^2}$$

If the given column is loaded only to the Point B', and we suppose that loading takes place at a temperature high enough to cause creep, the column will undergo a uniform compressive creep. A question which arises naturally is: Will the column in time become unstable in the straight form.

Referring to Figure 34, it is seen that, after an interval of time, the stress and strain will be given by the Point A'', because of the compressive creep which has taken place. If we suppose that loading is again resumed at A'', the loading curve will rise above A''. Let this loading curve be indicated by the dashed curve.

If it is assumed that the loading curve above A'' is independent of the creep that has occurred, the column will be as stable at A'' as it was at B' since  $E_t(A'')$  would then equal  $E_t(B')$  and the ratio

$$\frac{\sigma}{E_t}$$

would be the same at A'' as at B'.

If creep affects the prescribed loading in such a manner as to cause to decrease with increasing creep, it is possible that a point such as A''

might exist for which the ratio

$$\frac{\sigma(A'')}{E_t(A'')}$$

will equal

$$\frac{\sigma(A')}{E_t(A')}$$

Should this condition exist for the loading prescribed, the column would become unstable in the straight form at A'' in the same sense that it would have become unstable at A'. The value that  $E_t(A'')$  must have for this condition to be fulfilled can be determined from the fact that

$$\frac{\sigma(A'')}{E_t(A'')} = \frac{\sigma(A')}{E_t(A')} = \frac{\pi^2}{(L/r)^2}.$$

It follows from this that  $E_t(A'')$  must equal

$$\frac{(L/r)^2 \sigma(A')}{\pi^2}$$

if the column is to become unstable in the straight form at A''.

Although the above speculation might be of interest, it should be noted that, for a perfect column creeping under a constant load, it does not apply since the load does not increase after a time as was prescribed above. Since this is the case, any transition from the straight to the bent form must take place under a constant load. Because of this action, the ratio that must be satisfied eventually if the column is to become unstable in the straight form is

$$\frac{\sigma}{E_r} = \frac{\pi^2}{(L/r)^2}$$

If the Point A'' satisfied the ratio involving the tangent modulus, a point such as C'' might satisfy the above ratio. Proceeding as previously, the value of  $E_r(C'')$  can be found from the necessary condition that

$$\frac{\sigma(C'')}{E_r(C'')} = \frac{\sigma(C')}{E_r(C')} = \frac{\pi^2}{(L/r)^2}$$

From this, it follows that it is necessary that

$$E_r(C'') = \frac{(L/r)^2}{\pi^2} \sigma(C'').$$

Lest confusion arise from the fact that, in the preceding discussions, it was found that both  $E_r$  and  $E_t$  must equal the same value, it should be noted that the value of  $E_r$  depends on the shape of the column cross section. For a rectangular cross section, for example,

$$E_r = \frac{4E E_t}{[\sqrt{E} + \sqrt{E_t}]^2}$$

The foregoing discussion indicates that a perfectly straight column subject to creep at a load less than the tangent modulus load will not become unstable if the tangent modulus at a given stress level is independent of the creep that has occurred. If the tangent modulus decreases with increasing creep, the column can become unstable, and the criterion for instability will be given by the reduced modulus relation.

## APPENDIX II

### Creep of an Imperfect Column

A method of describing mathematically the creep of imperfect slender columns has been developed. The method is an extension of Popov's method which was formulated to describe the creep behavior of a beam subjected to pure bending.

In order to simplify the problem of column creep, several assumptions have been made. They are as follows:

1. Plane sections of the column cross section remain plane during bending.
2. The column material has a constant elastic modulus during creep.
3. The initial unloaded shape of the column can be described by a half sine wave.
4. The shape of the column during creep remains sinusoidal in form.
5. The effects of shear stress are considered negligible.
6. The column cross section is rectangular in shape.

The column to be considered is shown in Figures 35 and 36. For purposes of clarity, these figures are considerably exaggerated.

The unloaded configuration of the column,  $y_0$ , is given by the relation

$$y_0 = a_0 \sin \frac{\pi x}{L}$$

The terms in this relation are defined in the sketch of Figure 35.

The deflection due to a load,  $P$ , at the instant of application (time  $t = 0$ ) is

$$y_1 = \frac{a_0}{P_c/P - 1} \sin \frac{\pi x}{L}$$

where

$$P_c = \frac{\pi^2 EI}{L^2}$$

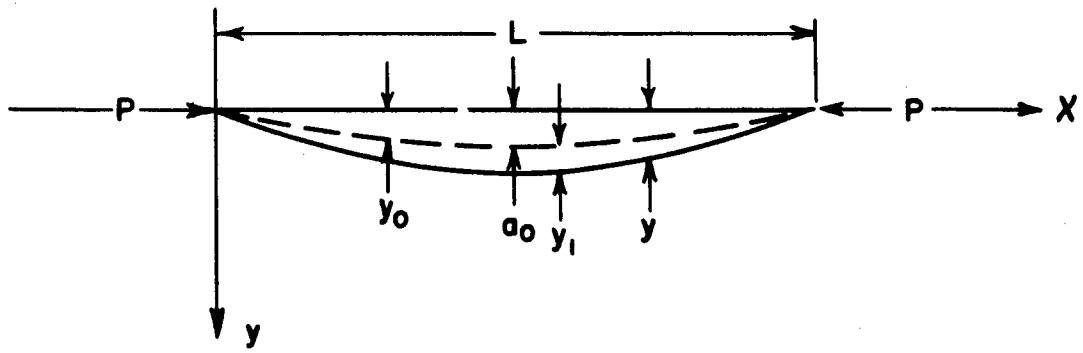


FIGURE 35. THE COLUMN CONFIGURATION

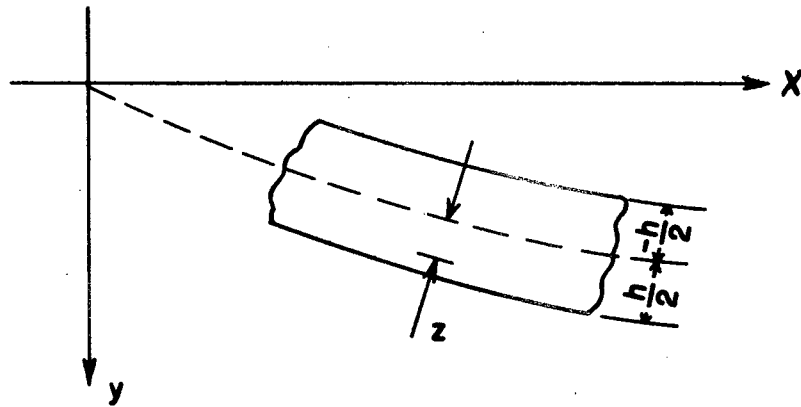


FIGURE 36. A COLUMN SECTION

and  $E$  is Young's modulus,

$I$  is the moment of inertia of the column cross section about the bending axis, and

$L$  is the column length.

At  $t = 0$ , the moment,  $M$ , at any cross section is

$$M = Py = P \left[ \frac{\sigma_0}{1 - P/P_c} \right] \sin \frac{\pi x}{L}$$

and the corresponding stress distribution is

$$\sigma_0 = \frac{-P}{A} + \frac{Mz}{I}$$

where  $A$  is the area of the column cross section, and  $z$  is the distance of a given point in the cross section from the axis, as shown in Figure 36.

The strain distribution at  $t = 0$  is

$$\epsilon_0 = \frac{-P}{EA} + \frac{Mz}{EI}$$

The forms of the initial stress and strain distributions are shown in Figures 37 and 38.

Due to the variable stress,  $\sigma_0$ , creep of different amounts will take place during a small, time interval from  $t = 0$  to  $t = t_1$ . Since the magnitude of the creep that occurs at a given point in the cross section depends on the stress level at the point, the resulting strain distribution will appear as  $\epsilon_1$  in Figure 38. If the creep behavior of the column material can be represented by an analytical relation, such as

$$\epsilon = f(\sigma, t)$$

the function  $\epsilon_1$  described above would be

$$\epsilon_1 = \epsilon_0 + f(\sigma_0, t_1)$$

The form of  $\epsilon_1$  violates the assumption about plane sections remaining plane, however, so  $\epsilon_1$  must be altered elastically to  $\epsilon_2$  as shown in Figure 40 to maintain the assumption. At this point, it should be noted that all of the adjustments made step by step in this development actually accompany one another continuously.

The adjustment from  $\epsilon_1$  to  $\epsilon_2$  can be accomplished by adding a variable stress  $(\sigma_2 - \sigma_0)$ , which is given by

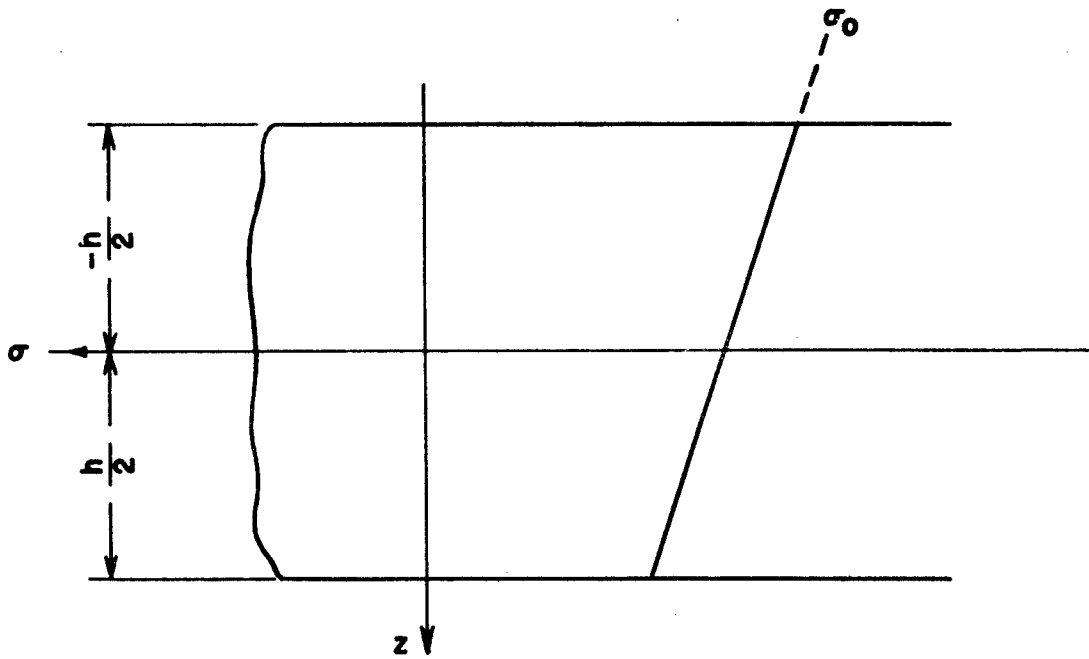


FIGURE 37. INITIAL STRESS DISTRIBUTION

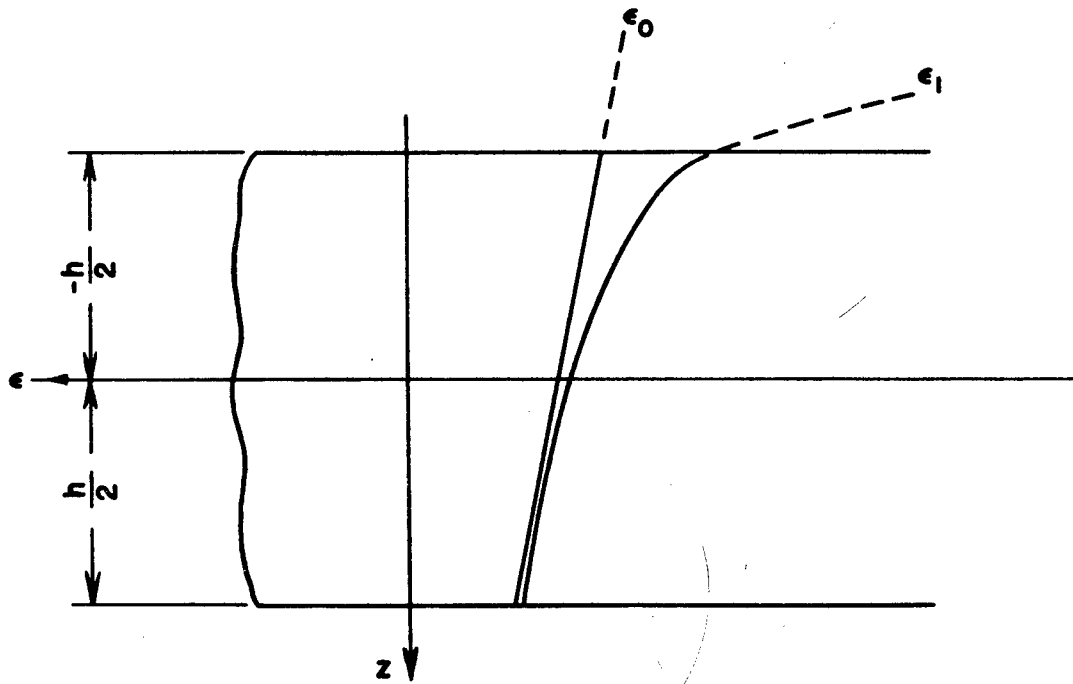


FIGURE 38. CHANGE IN STRAIN DUE TO CREEP

$$(\sigma_2 - \sigma_0) = E(\epsilon_2 - \epsilon_1)$$

The completion of this adjustment yields the stress distribution  $\sigma_2$  of Figure 39 and the strain distribution  $\epsilon_2$  of Figure 40.

Now plane sections originally plane are again plane, but it will be noted that a summation of forces in the  $x$  direction will yield the inequality

$$b \int_{-h/2}^{+h/2} \sigma_2 dz \neq b \int_{-h/2}^{+h/2} \sigma_0 dz = -P.$$

Since the inequality cannot exist, a constant, axial, elastic adjustment  $(\sigma_3 - \sigma_2)$  must be made. The magnitude of this adjustment can be obtained from the fact that it is necessary that

$$-P = b \int_{-h/2}^{+h/2} (\sigma_3 - \sigma_2) dz + b \int_{-h/2}^{+h/2} \sigma_2 dz.$$

Since  $(\sigma_3 - \sigma_2)$  is constant,

$$(\sigma_3 - \sigma_2) = -\frac{1}{h} \int_{-h/2}^{+h/2} \sigma_2 dz = -P/bh.$$

In this expression the integral must, of course, be evaluated by numerical integration.

The stress distribution,  $\sigma_3$ , after this adjustment appears as in Figure 41.

Corresponding to the stress alteration, there is an elastic-strain change given as

$$(\epsilon_3 - \epsilon_2) = \frac{(\sigma_3 - \sigma_2)}{E}.$$

This change is illustrated in Figure 42.

Now a balance of internal and external forces has been obtained, and all that remains is a moment check. The internal moment,  $M_i$ , at this stage is

$$M_i = b \int_{-h/2}^{+h/2} \sigma_3 z dz.$$

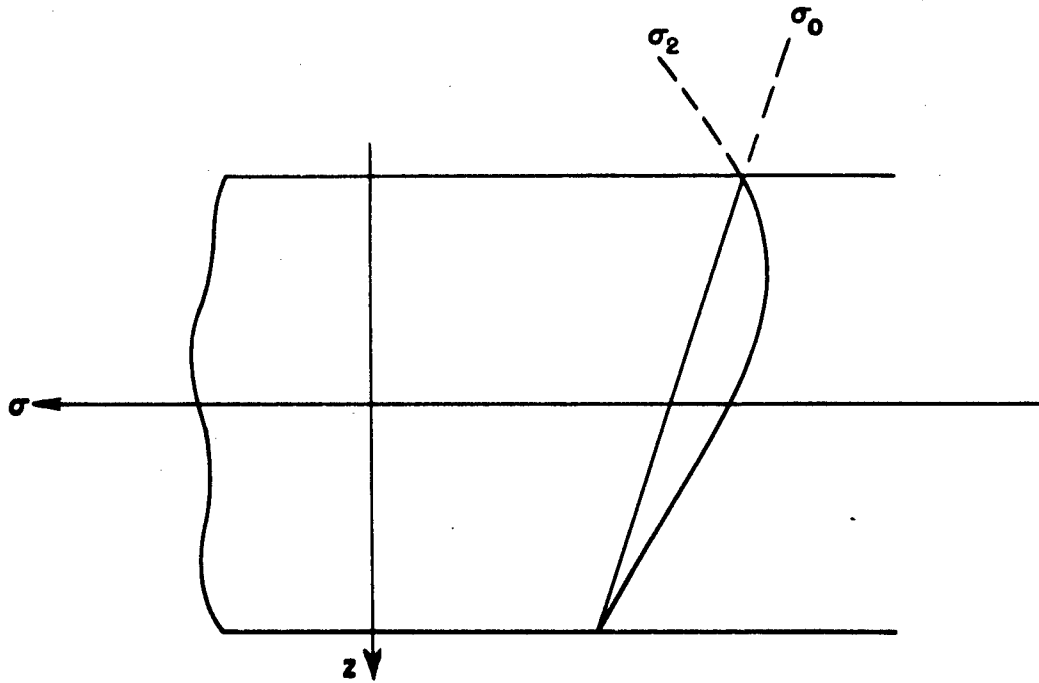


FIGURE 39. ELASTIC ADJUSTMENT TO OBTAIN PLANE SECTIONS

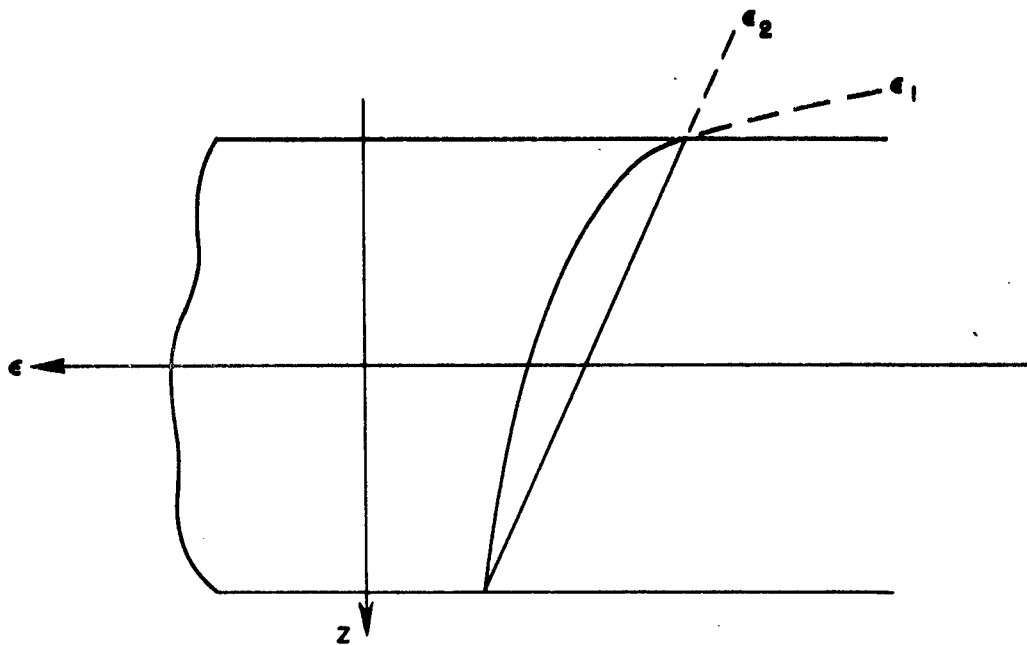


FIGURE 40. ELASTIC-STRAIN CHANGE TO OBTAIN PLANE SECTIONS

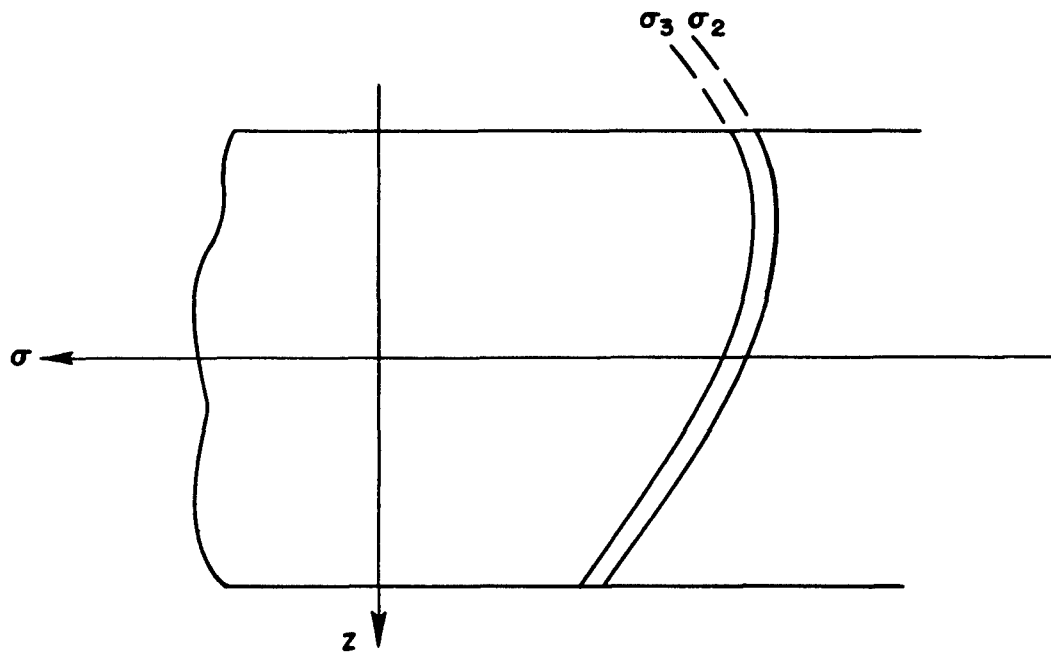


FIGURE 41. ELASTIC-AXIAL-STRESS ADJUSTMENT

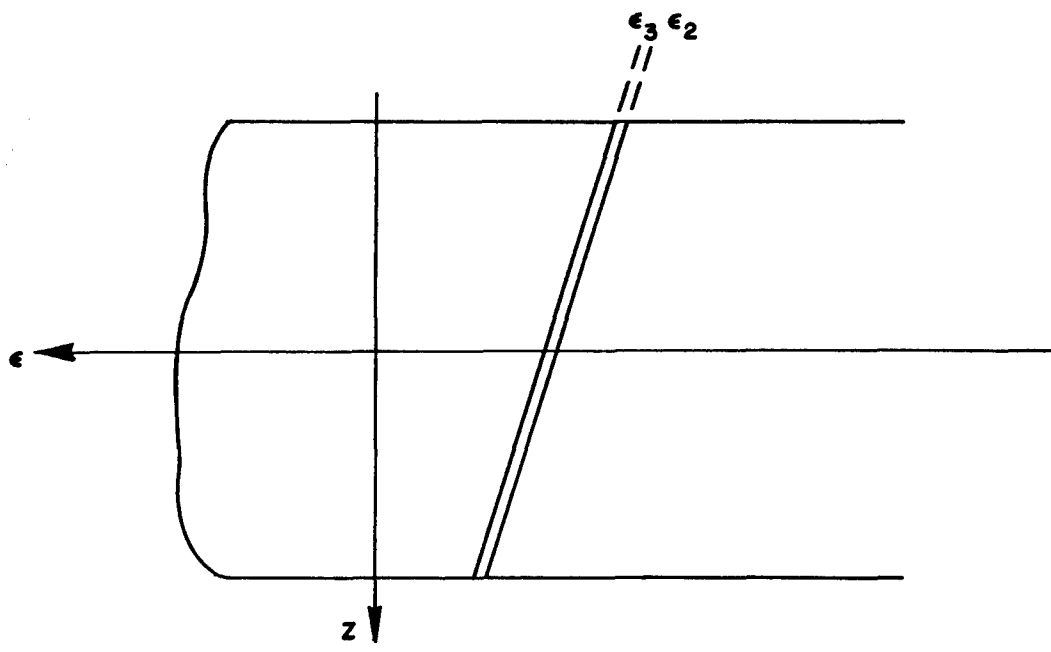


FIGURE 42. ELASTIC-AXIAL-STRAIN ADJUSTMENT

The external moment,  $M_e$ , is

$$M_e = Py.$$

At this point, the fourth assumption will be introduced in order to simplify the analysis. Let it be assumed that the deflection curve at any time,  $t$ , is

$$y = y_0 + y_1 = y_0 + c(t) \sin \frac{\pi x}{L}.$$

Using this assumption, it follows that

$$C(t) = \frac{L^2}{\pi^2 h} [\epsilon_v - \epsilon_c].$$

where

$\epsilon_v$  is the strain on the convex face at  $x = L/2$ , and

$\epsilon_c$  is the strain on the concave face at  $x = L/2$ .

Making use of this value for  $C(t)$ ,  $y$  becomes

$$y = y_0 + \frac{L^2}{\pi^2 h} [\epsilon_v - \epsilon_c] \sin \frac{\pi x}{L}$$

Since the form of the deflection curve is now prescribed, it is only necessary to consider the action at one cross section. In all further calculations, only the cross section at  $x = L/2$  will be considered.

For  $x = L/2$ ,

$$y = a_0 + \frac{L^2}{\pi^2 h} [\epsilon_v - \epsilon_c].$$

For the strain distribution  $\epsilon_3$ , the value of  $M_e$  for  $x = L/2$  is

$$M_e = P \left[ a_0 + \frac{L^2}{\pi^2 h} (\epsilon_3 (h/2) - \epsilon_3 (-h/2)) \right].$$

Since  $M_e$  is not likely to be equal to  $M_i$ , an elastic-bending adjustment giving a final stress of  $\sigma_4$  and a final strain of  $\epsilon_4$  must be made. This final adjustment must be such that the condition

$$P \left[ a_0 + \frac{L^2}{\pi^2 h} (\epsilon_4 (h/2) - \epsilon_4 (-h/2)) \right] = b \int_{-h/2}^{+h/2} \sigma_4 z dz$$

is satisfied.

If this moment balance is rewritten in the form

$$P \left\{ a_0 + \frac{L^2}{\pi^2 h} [\epsilon_3(h/2) - \epsilon_3(-h/2)] + \frac{L^2}{\pi^2 h} [(\epsilon_4(h/2) - \epsilon_3(h/2)) - (\epsilon_4(-h/2) - \epsilon_3(-h/2))] \right\} = b \int_{-h/2}^{+h/2} \sigma_3 z dz + b \int_{-h/2}^{+h/2} (\sigma_4 - \sigma_3) z dz,$$

the adjustments  $(\sigma_4 - \sigma_3)$  and  $(\epsilon_4 - \epsilon_3)$  become apparent. These adjustments are as shown in Figures 43 and 44.

Since this adjustment is an elastic bending, the following relationships can be utilized:

$$(\epsilon_4 - \epsilon_3) = \frac{(\sigma_4 - \sigma_3)}{E}.$$

$$(\sigma_4 - \sigma_3) = \frac{2z}{h} (\sigma_4(h/2) - \sigma_3(h/2)).$$

Making use of these relationships yields

$$P \left\{ a_0 + \frac{L^2}{\pi^2 h} [\epsilon_3(h/2) - \epsilon_3(-h/2)] \right\} + \left[ \frac{2PL^2}{\pi^2 h E} - \frac{2I}{h} \right] (\sigma_4(h/2) - \sigma_3(h/2)) = b \int_{-h/2}^{+h/2} \sigma_3 z dz.$$

Solving this expression for  $(\sigma_4(h/2) - \sigma_3(h/2))$  gives

$$(\sigma_4(h/2) - \sigma_3(h/2)) = \frac{h}{2I [P/P_c - 1]} \left\{ b \int_{-h/2}^{+h/2} \sigma_3 z dz - P \left[ a_0 + \frac{L^2}{\pi^2 h} (\epsilon_3(h/2) - \epsilon_3(-h/2)) \right] \right\}.$$

In Figure 43, the curve for  $\sigma_4$  is indicated as being an increase in the compressive stress on the  $z = -h/2$  face, and a decrease or unloading on the  $z = h/2$  face. Intuitively, this is what might be expected, since the creep that took place earlier in the development created an increase in the moment arm, and, therefore, should have been accompanied by an additional elastic bending.

From the expression for the final stress adjustment at  $z = h/2$ , the general adjustment  $(\sigma_4 - \sigma_3)$  can be determined from the equation

$$(\sigma_4 - \sigma_3) = \frac{2z}{h} (\sigma_4(h/2) - \sigma_3(h/2)).$$

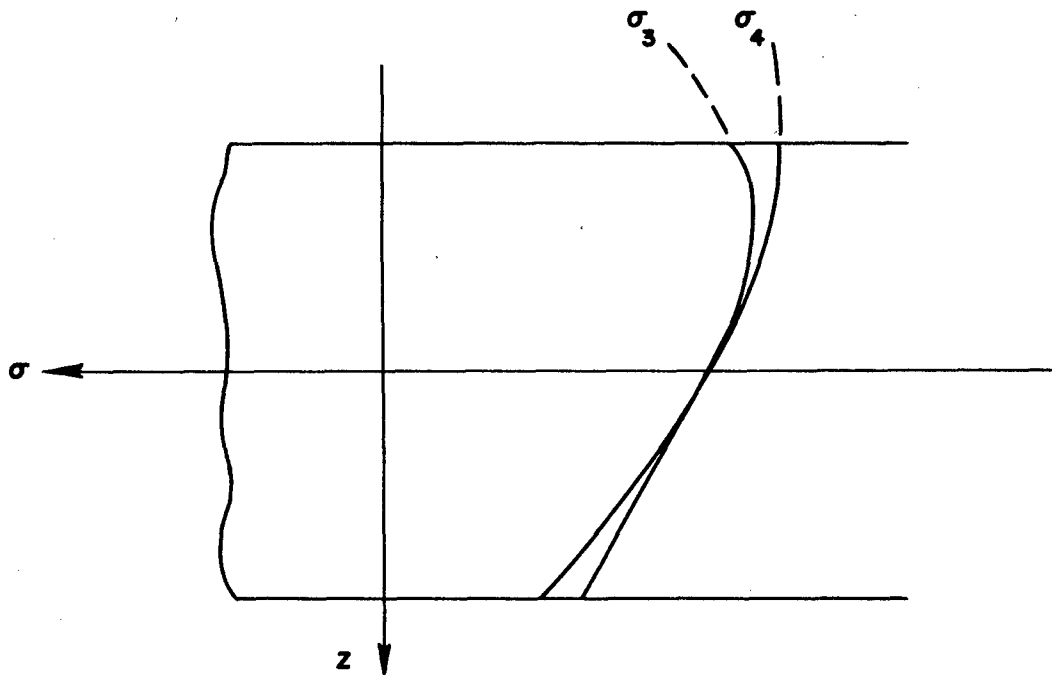


FIGURE 43. ELASTIC-BENDING-STRESS ADJUSTMENT

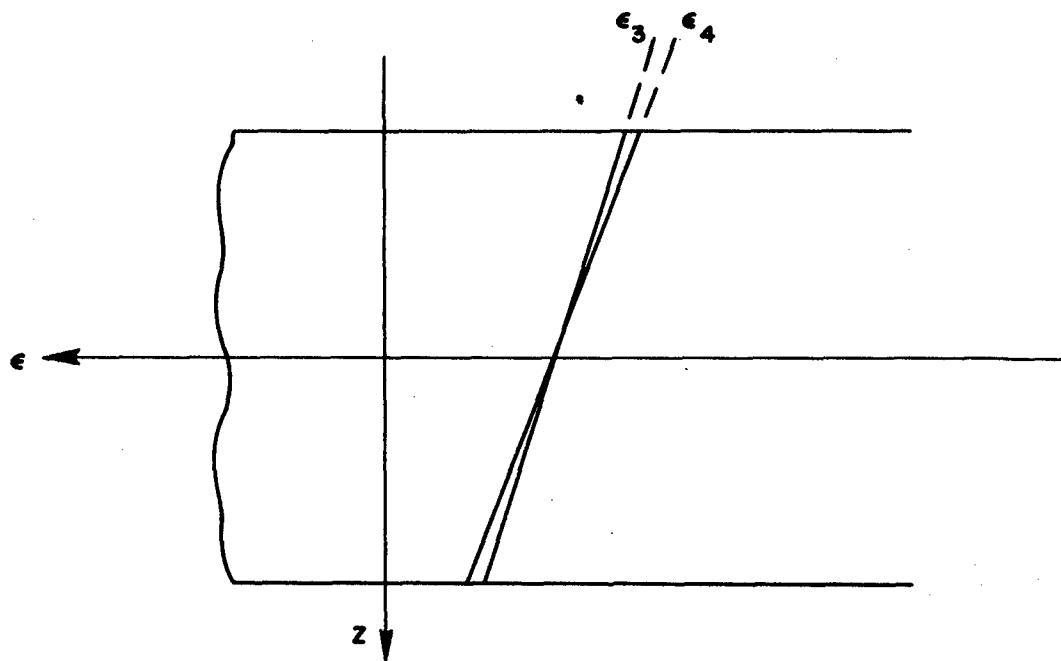


FIGURE 44. ELASTIC-BENDING-STRAIN ADJUSTMENT

The final strain adjustment is

$$(\epsilon_4 - \epsilon_3) = \frac{(\sigma_4 - \sigma_3)}{E}$$

and the deflection,  $y$ , at the end of the first time interval will be

$$y(x, t_1) = \left[ a_0 + \frac{L^2}{\pi^2 h} (\epsilon_4(h/2) - \epsilon_4(-h/2)) \right] \sin \frac{\pi x}{L},$$

or for  $x = L/2$ ,

$$y(L/2, t_1) = \left[ a_0 + \frac{L^2}{\pi^2 h} (\epsilon_4(h/2) - \epsilon_4(-h/2)) \right].$$

To give an idea of the type of change that might occur during the time interval from  $t = 0$  to  $t = t_1$ , the initial and final stress and strain distributions are given in Figures 45 and 46.

To obtain deflections for the time interval beyond  $t = t_1$ , it will be necessary to repeat the above calculations using  $\sigma_4$  as the starting stress distribution.

The creep which will occur during this new time interval can be determined by the use of the strain-hardening assumption, which assumes that creep rate is a function of the variable stress and creep strain. Since the description and utilization of this assumption has been clearly described in the literature<sup>(5, 6)</sup>, further discussion here is not deemed necessary.

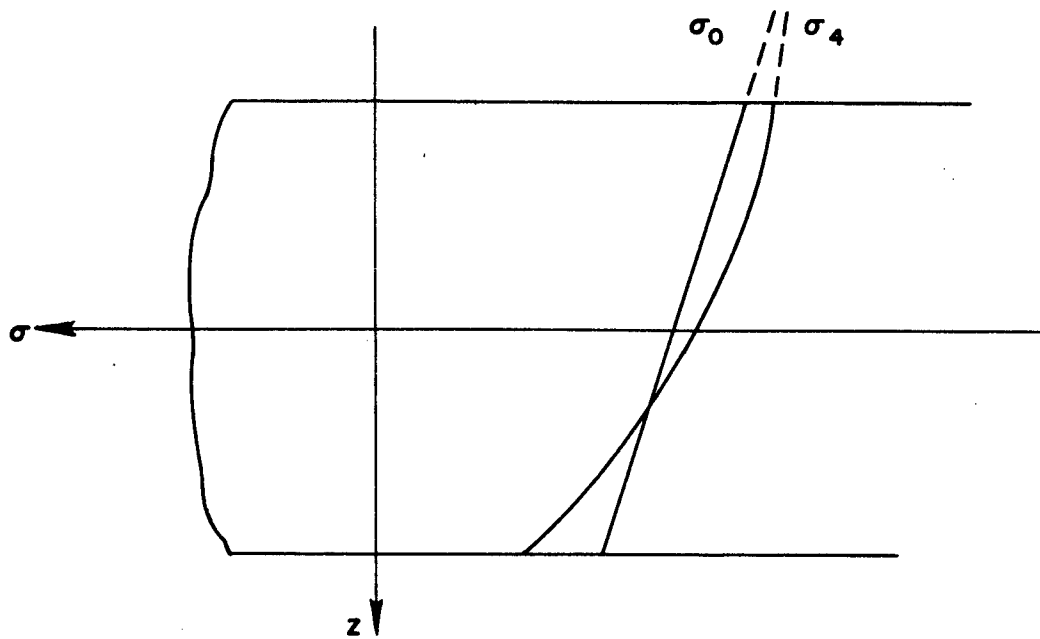


FIGURE 45. INITIAL AND FINAL STRESS DISTRIBUTIONS

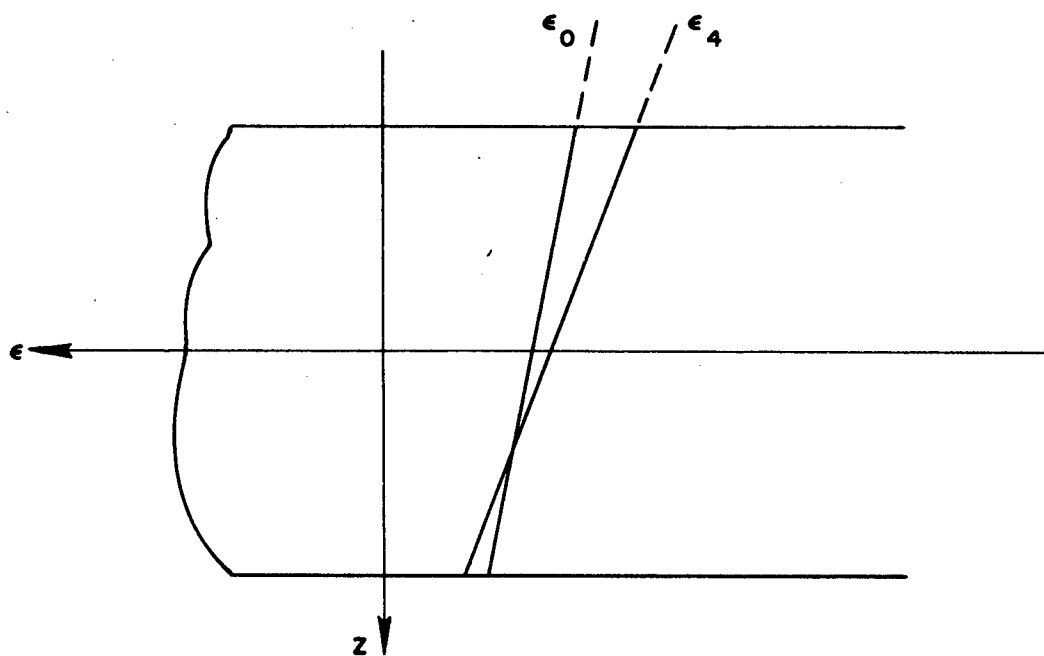


FIGURE 46. INITIAL AND FINAL STRAIN DISTRIBUTIONS